A Study of Interference Fields in a Ducting Environment

George A. Hufford
Donald R. Ebaugh, Jr.

TABLE OF CONTENTS

LIST OF FIGURES

A Study of Interference Fields in a Ducting Environment

George A. Hufford and Donald R. Ebaugh, Jr.*

In a cooperative program, the Federal Communications Commission and the Institute for Telecommunication Sciences have begun a study of the interference fields that may arise in a ducting environment. This report gives some preliminary thoughts on how enhanced signal levels might be modeled and describes a measurement program that operated in Southern California. Comparisons are made between some of the first-order statistics of the data and two of the possible models and show that there still remains a large gap between our modeling abilities and reality.

Key words: long-term variability; radio ducts; radio propagation; short-term variability; UHF; VHF

1. INTRODUCTION

In some regions of the world, ducting phenomena are fairly common and lead to interference at surprisingly long distances. To allow better spectrum management, we need to be able to foretell on what propagation paths such long-range interference is likely to happen. This information is essential in managing the broadcast services and the mobile services when one must choose frequency assignments, base station and transmitter locations, and permissible radiated powers and antenna heights.

As a start toward satisfying this need, the Institute for Telecommunication Sciences (ITS) has entered into a cooperative program with the Federal Communications Commission (FCC) to acquire data related to these phenomena, to assemble the resulting statistics, and to try to determine a widely applicable model. A part of these efforts involves a measurement program that originally observed received signal levels on long paths in southern California. The paths extend from Los Angeles to San Diego and are in a region well known for the persistent occurrence of super-refractive layers.

This report gives some preliminary ideas concerning the ultimate model, describes some of the first-order statistics of the data obtained from the measurement program, and provides a comparison of these statistics with candidate models.

---

*The authors are with the Institute for Telecommunication Sciences, National Telecommunications and Information Administration, U.S. Department of Commerce, Boulder, CO 80303.

2. POSSIBLE APPROACHES TO MODELING

In attempting to describe the effect of the atmosphere on radio waves, one very straightforward approach is to measure the refractivity structure and then to trace rays or to perform a modal analysis for that structure. Such an approach is actually used today as a real-time technique--by the Navy, for example, to provide a better interpretation of radar returns (see Shkarofsky and Nickerson, 1982), and by NASA to improve the accuracy of range finders. The method is expensive and, as it turns out, still of questionable accuracy. Its biggest drawback, however, is that it provides only a snapshot of the conditions and cannot be directly used for planning purposes.

If we are to have a less expensive, more generally applicable method, we must devise a model for the statistics of received signal levels. Actually, we need two models: one to describe the atmosphere and another to describe the effects of the atmosphere on radio waves. Since the first of these will provide part of the input data to the second, it needs to model only those characteristics of the atmosphere that the second model requires. On the other hand, the second model should not require more data concerning the atmosphere than can be conveniently modeled from meteorological considerations. There is a tight interplay between the two.

There have been many attempts to provide suitable models of the atmosphere. The most recent (and probably most promising) has been that of Dougherty and Dutton (1981). In what follows here, we shall concentrate on the second part of the modeling--the relationship between the atmosphere and received signal levels.

Because the atmosphere changes at the whim of the notoriously hard-to-predict weather, our only choice is to assume that the received signal level on any particular path is to be considered a random process $w(t)$. For future convenience, we measure this in decibels relative to any desired level (1 mW, for example, or 1 μV/m--even the units used are not important for our purposes). And we use the lower-case letter to indicate it is a random variable. Statistics of the process will be indicated by upper-case or Greek letters.

It is customary to separate the signal level process into two superimposed processes. One represents the small-scale or short-term variability, while the other represents the large-scale or long-term variability. The principal reason for this separation is that the two normally arise from different physical causes. The short-term variability is

usually due to multipath fading--when there are two or more components of the radio field that arrive at the receiving terminal by way of separate paths and so add together vectorially according to their relative phases. The observed variations with time come about because minute variations in the atmosphere will change the electrical lengths of the several paths and so change the relative phases. Long-term fading, on the other hand, is caused by wide-scale changes in the atmosphere that affect the number and the magnitudes of the multipath components. Since one expects gross changes in the atmosphere during the course of the day, it is common to use the period of one hour to distinguish the two processes. Thus, one also speaks of the within-the-hour and the hour-to-hour variations.

In formal terms we may write

$$w(t) = w_0(t) + r(t) \tag{1}$$

where $w_0(t)$ is a "smoothed" version of the received signal level (usually "hourly medians") and the residual $r(t)$ represents the small-scale variations. As indicated by the lower-case letters, both components are to be treated as random processes; w_0 is measured in the same units as is w, and r is measured in simple decibels. Since $w_0(t)$ will equal the local median value, r will always have a median value of 0 dB.

The form of (1) implies a multiplicative relation for the corresponding amplitudes or powers. This is by design. If the short-term variations are caused by multipath, then they may also be called "frequency-selective fading." If at any instant we were to examine the received signal level over a wide band of frequencies, we would find a very similar kind of variability in which $w_0(t)$ provides an overall, general level. From the point of view of the resulting frequency transfer function, it would be quite proper to multiply the general level by a normalized random function of frequency.

2.1. Short-term Variability

In the case of short-term variability there are some simple considerations that already allow us to reach fairly concrete results. These considerations rest on the assumption that this variability is caused, as stated above, by multipath fading in which the phases of received components vary because of minute variations in the refractivity of the atmosphere. Statistics of the short-term variability then depend only on the number of components and on their relative magnitudes.

3
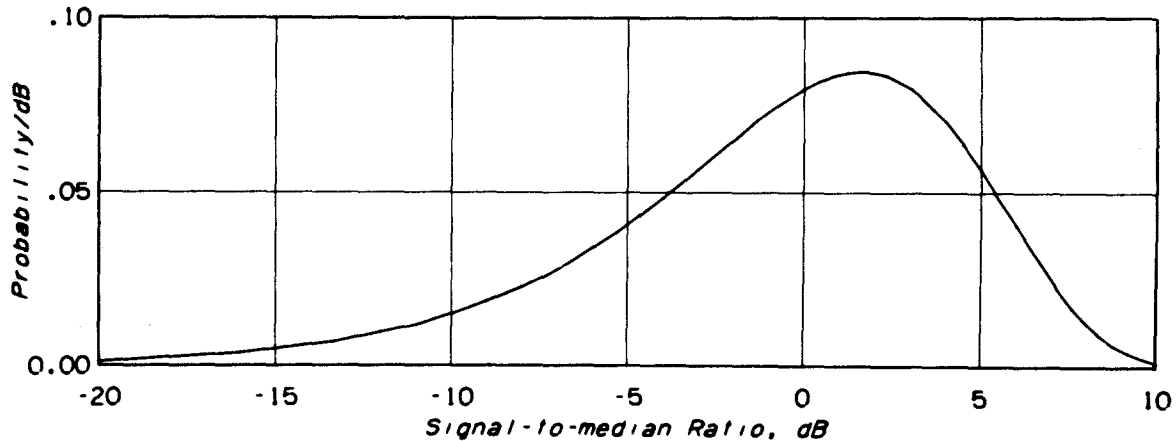
Figure 1. The density function of the Rayleigh decibel distribution.

First, let us suppose there are many components, none of which predominate. Then we have the case of Rayleigh fading (see, e.g., Rayleigh, 1894). The received signal is the vector sum of several voltages having nearly the same amplitude but entirely random phases. The first-order statistics (those that depend only on a single instant of time and do not measure how rapidly the signal varies) satisfy the Rayleigh Law. For the quantity r, the (complementary) cumulative distribution is given by the simple formula

$$q = Pr[r > R] = 2^{-10^{R/10}} \tag{2}$$

We might call this the Rayleigh decibel distribution since the term "Rayleigh distribution" is usually restricted to the distribution of the underlying voltage amplitudes. Solving (2) for R we obtain the quantile

$$R(q) = 10 \log \frac{\ln 1/q}{\ln 2} \tag{3}$$

so that R(q) is the value that r exceeds for the fraction q of the time. Note that this distribution has no parameters, a fact that makes it easy to use since no measurements to determine parameters are necessary. It has a mean of 0.92 dB, a standard deviation of 5.57 dB, and an interdecile range Δr = R(0.1) - R(0.9) = 13.40 dB. In Figure 1 we have plotted its density function--the negative derivative of (2). The resulting bell-shaped curve is skewed toward the negative values.

4

Of course, it is more common in the literature to introduce a nonzero median as a simple parameter of the Rayleigh distribution. In our notation this is done by simply adding that median to the right-hand side of (3); here, this addition is taken care of already in (1) by the local median term w_o.

When the multipath components do not satisfy the simple requirements for Rayleigh fading, the next condition one can assume is that there are still several components present but that one of them is much stronger than the others. This condition leads to first-order statistics that satisfy what is known as the Nakagami-Rice distribution (and also the Ricean or the "constant-plus-a-Rayleigh" distribution; see, e.g., Norton et al., 1955). Aside from the median (which here we shall want to assume vanishes), it has one parameter that can be represented as C, the "constant-to-scattered" ratio measured in decibels. This is the ratio of the power in the single strong component (the "constant" component) to the average power in the sum of the remaining components (the "scattered" component). It is interesting to note that, except for a slight change in meanings of the variables and parameters, the Rayleigh distribution is equivalent to the chi-squared distribution with two degrees of freedom. Similarly, the Nakagami-Rice distribution is equivalent to the "noncentral" chi-squared distribution with two degrees of freedom. Both of these distributions are described in, e.g., Abramowitz and Stegun (1964), and computer programs to calculate values may be found in some of the available libraries of mathematical or statistical functions. In any case, however, statistics of the Nakagami-Rice distribution are hard to compute and they depend on the parameter C in a nontrivial way.

In studies of short-term variability, it is customary to plot observed cumulative distributions on "Rayleigh paper." This is graph paper in which the ordinate represents the received signal level scaled linearly in decibels, and the abscissa represents probability (or fraction of time) scaled nonlinearly according to the negative of the right-hand side of (3). If a distribution satisfies the Rayleigh Law, then it will appear on Rayleigh paper as a straight line with slope -1.

On the other hand, if we used Rayleigh paper to plot the Nakagami-Rice distribution, we obtain results such as those portrayed in Figure 2 where the several curves correspond to several values of the parameter C. The most
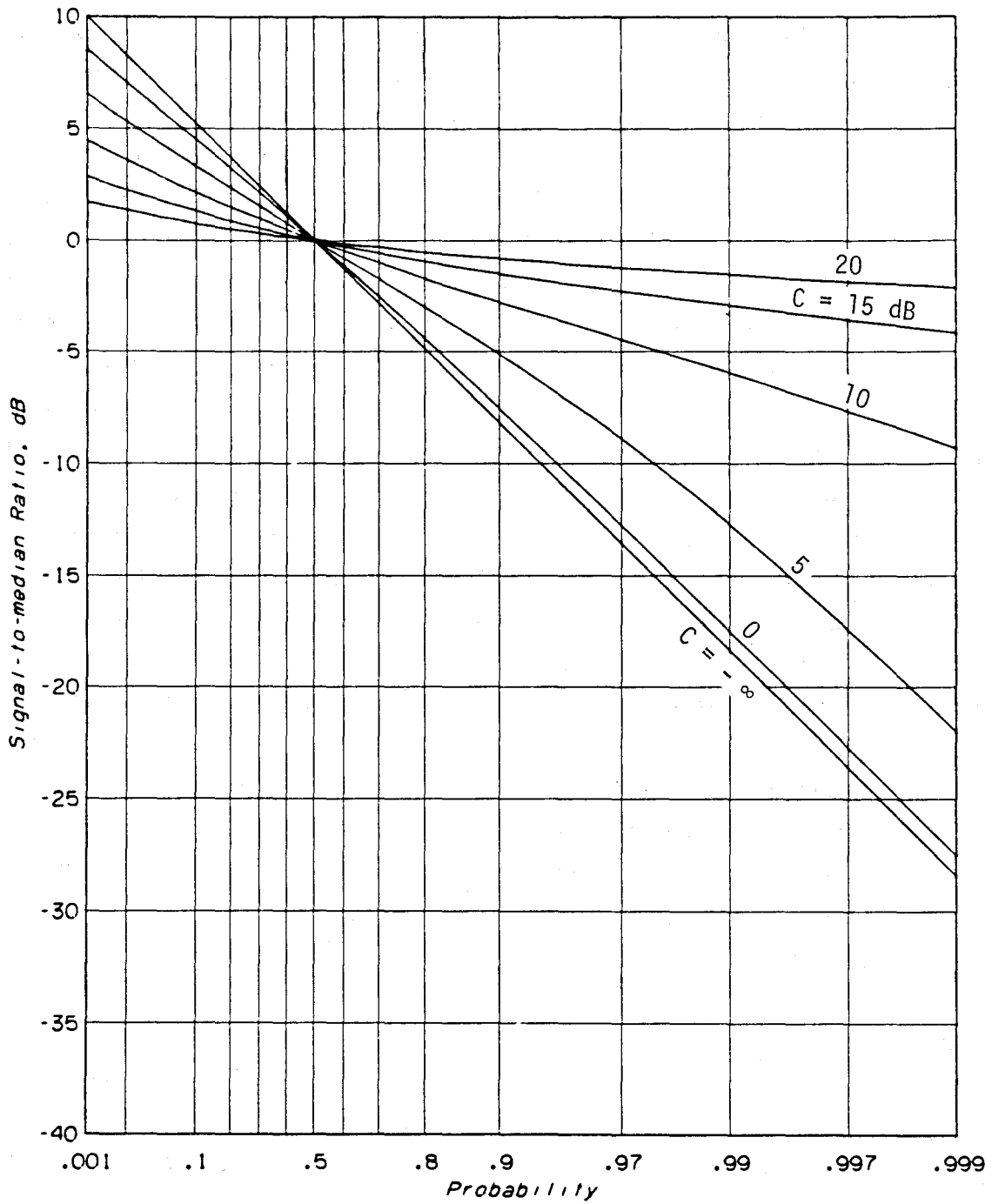
5

Figure 2. Nakagami-Rice distributions drawn on Rayleigh paper. The parameter C is the constant-to-scattered ratio in decibels.

6

striking thing about these curves is that they all look like straight lines; so much so that replacing them by straight lines appears to be a reasonable approximation.

Now as it happens there is a distribution used in the theory of reliability known as the Weibull distribution, which may be most simply defined as one that plots out as a straight line of arbitrary slope on Rayleigh paper (Weibull, 1951). It seems very appropriate, then, to use this distribution as an approximation to the Nakagami-Rice distribution, the point being that many of its characteristics are easy to compute. If the slope equals $-\alpha$, then the quantiles are easily determined from (3) as

$$R(q) = \alpha \; 10 \; \log \frac{\ln 1/q}{\ln 2} \tag{4}$$

As with the Rayleigh distribution, we should probably call this the Weibull decibel distribution, since the usual definition is in terms of the amplitude. The mean, standard deviation, and interdecile range are all equal to the Rayleigh values multiplied by the slope α. Since the relation here is so simple and since the slope of a cumulative distribution is one measure of the "concentration," one may as well replace α as the parameter of the Weibull distribution by either the standard deviation or the interdecile range, both of which may have more immediate meanings. In what follows, we shall normally prefer the interdecile range Δr as the most convenient of these measures.

To remain within the range of the Nakagami-Rice distribution, the value of α should be restricted to lie between 0 and 1. At the extreme $\alpha = 0$, we have a simple jump distribution in which $r(t) = 0$ with probability 1. This corresponds to the case where there is only the isolated single component, the others having vanished. At the other extreme, $\alpha = 1$, we have the Rayleigh distribution again; here, the isolated component has vanished. For intermediate values there will be a nontrivial relation between the parameter C of the Nakagami-Rice distribution and the slope. In Figure 3 we have plotted the interdecile range of the Nakagami-Rice distribution versus C. This plot is, however, of only incidental interest since from a phenomenological point of view it is immaterial which of these related parameters we use and the interdecile range is certainly the easier to measure and to employ in further computations.
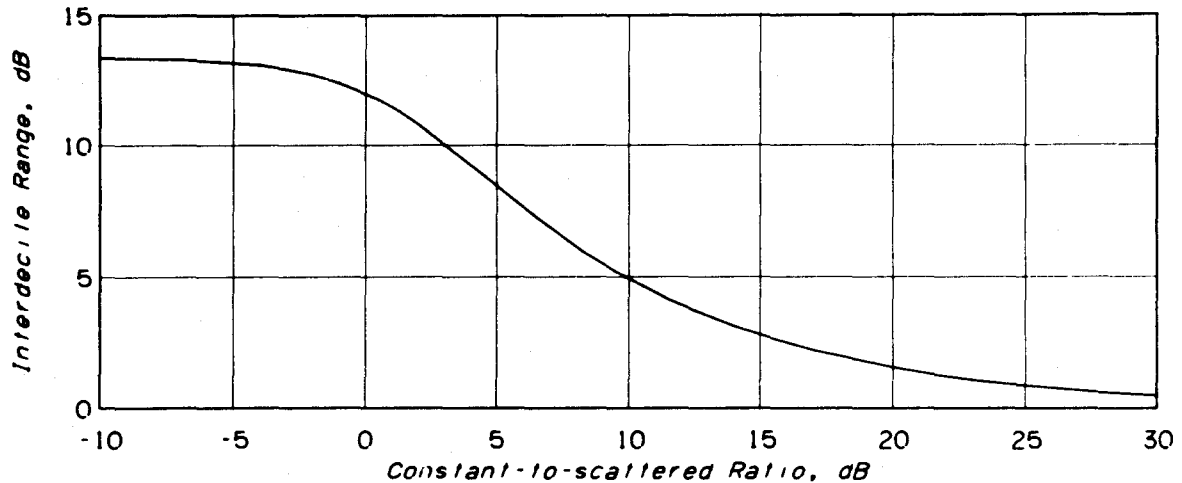
7

Figure 3. The interdecile range of the Nakagami-Rice distribution.

There is one other model of the first-order statistics of short-term variability that is sometimes mentioned in the literature (see, for example, Dougherty, 1968). Called the two-ray model, it assumes there are just two components in the multipath field with relative phases that are uniformly distributed over the whole circle. The resulting quantiles (in decibels) are given by

$$R(q) = 10 \log\left(1 + \frac{2\beta}{1 + \beta^2} \cos \pi q\right) \qquad (5)$$

where β is the (voltage) ratio between the amplitudes of the two components. In Figure 4 we have plotted a few of these distributions on Rayleigh paper using the parameter $B = 20 \log \beta$. In addition to flattening out in the tails, these distributions all show a strong downward curvature at central values. We might note that when B vanishes (so that the two components have equal magnitudes) the interdecile range is 16.01 dB. This is therefore one example of a distribution with a steeper average slope than that of the Rayleigh distribution. The difference, however, is small and when B exceeds only 2.5 dB, it vanishes.

Experience has shown that in the great majority of cases the Nakagami-Rice distribution (and especially the limiting case of the Rayleigh distribution) does indeed portray fairly accurately the observed first-order statistics of short-term fading. Until other distributions, such as that of
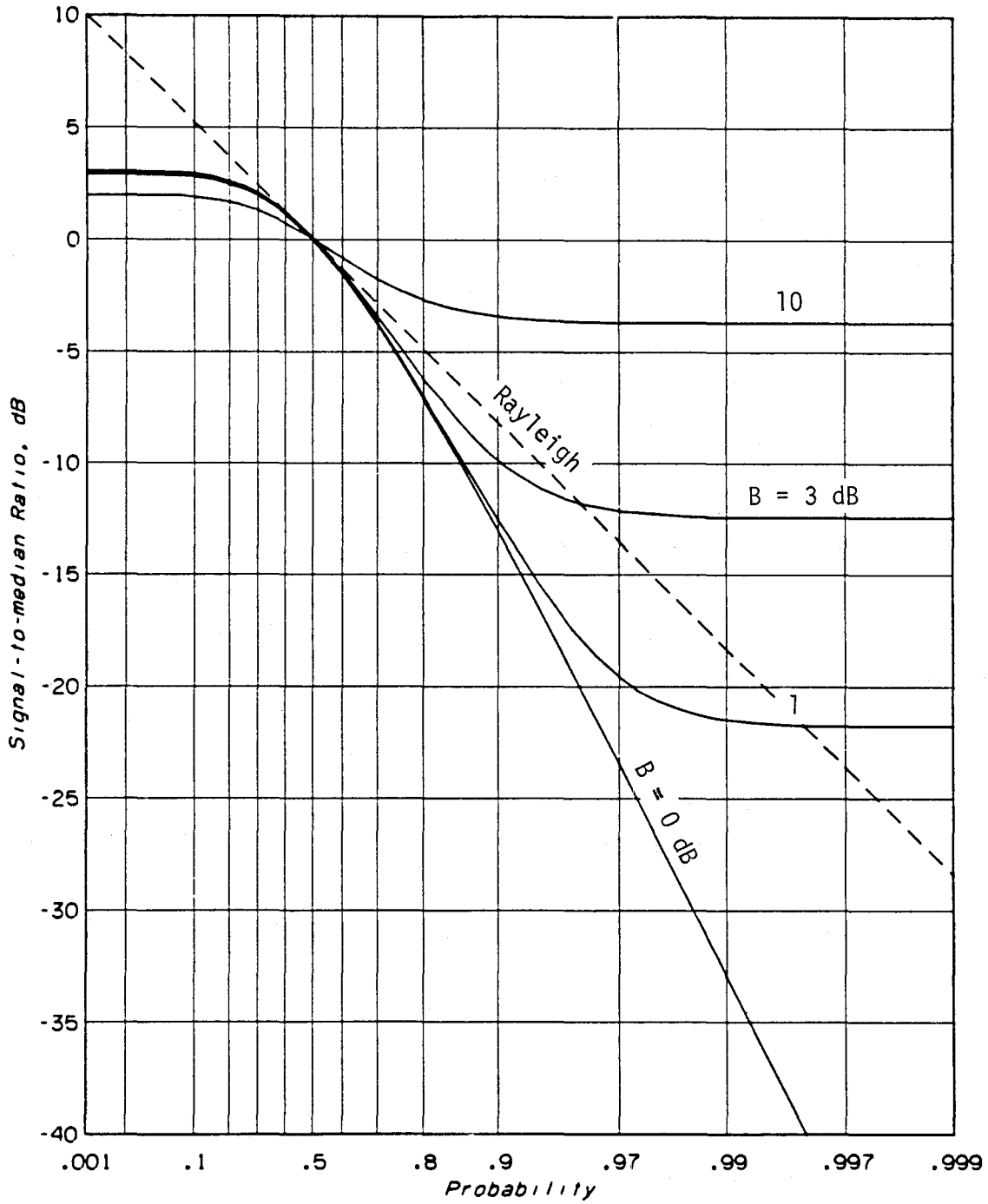
8

Figure 4. Distributions of the two-ray model drawn on Rayleigh paper. The parameter B is the ratio in decibels of the two amplitudes.

9

the two-ray model, are shown to be of importance, we would propose to model these statistics with this one set of distributions and, further, to replace them by the more easily managed Weibull approximations.

2.2 Long-Term Variability

We have seen, then, that within each hour the first-order statistics can be characterized by two parameters--the median and the interdecile range Δr. From hour to hour we would suppose that both parameters will vary and so we are led to consider two slowly varying random processes, $w_0(t)$ and $\Delta r(t)$, whose statistics are those of the long-term variability. Our first concern will be for the first-order statistics of these processes; but note that we would expect the two to be statistically dependent and also that they probably have diurnal and seasonal trends.

To study these statistics, we seem obliged to resort to an empirical study of measured data. Our present state of knowledge does not permit us to do much more, although certainly any modeling of the phenomena should take account of whatever we do know. There have been very few previous measurements of the within-the-hour interdecile range and an attempt to model its statistics must wait on the acquisition of a body of data. We turn here to a discussion of the hourly median.

Of past attempts at modeling long-term variability, probably the most widely used method is that suggested by Rice et al. (1967). It forms a part of the ITS Irregular Terrain Model (see Longley and Rice, 1968; and Hufford et al., 1982) and of a Comité Consultatif International des Radiocommunications (CCIR, 1978a) approach. In this method one writes

$$w_0(t) = W_{ref} + v(t) \tag{6}$$

where W_{ref} is a "reference" level and $v(t)$ is a "deviation." The reference level is meant to be the fixed signal one would obtain with a "normal" atmosphere--i.e., a hydrodynamically unstable (hence turbulent) atmosphere where the refractivity follows a fixed exponential decrease with increasing altitude. The deviation then forms a random process, and there is nothing new here. The important step, however, is to assume that the first-order statistics of the deviations can be described in terms of only two parameters--the "climatological type" and an "effective distance." The climatological type can be one of some eight discrete types ranging from "equatorial" to "polar." The effective distance is a function of actual

10

distance, frequency, and antenna heights; it is a normalized distance that attempts to put all paths into a common mold. In practice, one speaks of the median V(0.5) and of the quantiles of the deviations--which are now denoted by y(t)--from this median. In Figure 5, we show the curves of these quantiles versus effective distance for the case of the "maritime temperate over land" climate. Except for the design of the effective distance, such curves are entirely empirical; they have been drawn through measured values that exhibit, unhappily, a rather large spread.

Nevertheless, the method performs fairly well. This is attested to in the report by Longley et al. (1971), which summarizes data from a large number of paths and compares the observed cumulative distributions of hourly medians with those provided by this method.

The method was originally prepared to treat the case of those paths over which the dominant mode of propagation is tropospheric scatter. It was then extended to include shorter paths. Ducting phenomena, however, have never been satisfactorily included. In Figure 5, there are some large upswings at large effective distances for the very low percentiles. This represents an attempt to describe the enhanced fields that arise, presumably, from the presence of ducts. But this refers to the "normal" antenna towers in the presence of the "normal" duct heights that appear in a maritime temperate climate--which probably means the North Sea since that is the region used to epitomize this climatological type. There is no attempt made to allow for other situations. In general, we would suppose that pegging the enhanced fields caused by ducting to the "reference" level can never be satisfactory.

The method just described tries to portray the entire range of time variability. A second method--one that concerns only the enhanced fields present for very small fractions of time--was first suggested by Misme (1974) and is now a method given by the CCIR (1978b). It speaks of a "leakage coefficient" into and out of a presumed duct and of a "minimum coupling distance" into the duct. It gives a formula for the attenuation relative to free space directly without the mention of a reference level. The formula is most obviously a function of the path length but the coefficients involved depend on the average initial lapse rate of refractivity, the frequency, the terrain irregularity parameter Δh, and the proportion of the path that lies over sea. The method is designed for quantiles of 1% or less and for frequencies between 600 MHz and 15 GHz.
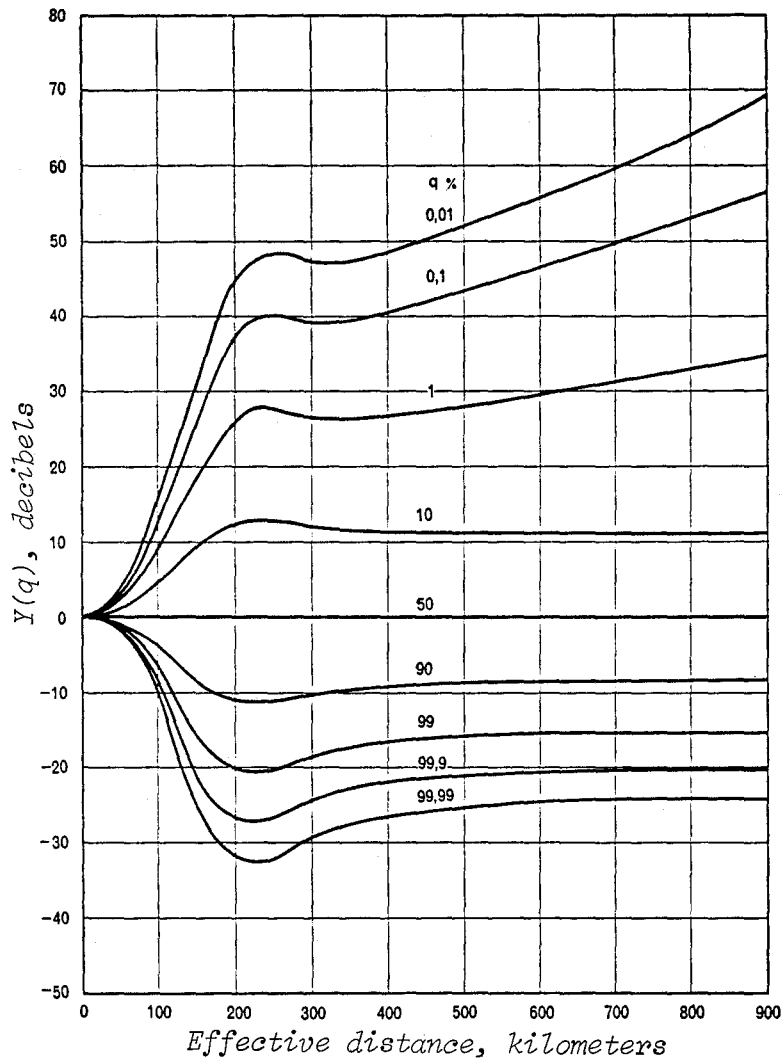
11

Figure 5. Quantiles of deviations versus effective distance for the
maritime temperate climate over land. Adapted from CCIR
(1978a).

This approach has many of the features that seem desirable to us; the limitations seem severe but could probably be relaxed with further study. On the other hand it seems a little artificial to use the average initial lapse rate of refractivity to categorize the incidence of ducts and their characteristics--other climatic parameters would probably be more suitable. Another parameter that is missing from the method is the antenna elevation and how it relates to the possible duct elevation; this seems important to us.

In general, we would expect signal levels in the presence of a duct to depend on the depth, strength, and extent of the duct and on the radio frequency and the path geometry. Thus, the statistics of signal enhancement will depend on these factors and on the frequency of occurrence of ducting layers. Path geometry is important because it is at grazing incidence upon a ducting layer when effects are most pronounced. As the ray elevation angle is increased from 0° to perhaps 5° (about 85 mrad) the effects become negligible. Enhancements can be as great as 40 dB above the long-term median for transhorizon paths. On line-of-sight paths (perhaps 50 km long) signal levels 6 dB above free space are not unknown.

If a radio transmitting antenna is _above_ a horizontal ducting layer, the usual effects are multipath fading and extended range while radio holes and antiholes may also occur. If the transmitter is _within_ the layer, extended range occurs along and below the layer so that if both transmitter and receiver are within the layer, an enhanced signal level may exceed the free space level for great distances. This can happen because within the duct there is an inverse distance dependence, while in free space the decrease in signal level is proportional to the square of the distance. If an elevated layer is very much _above_ the normal path of a radio ray, the duct will have little, if any, effect on propagation losses.

With these considerations in mind, we would suppose that a good, widely applicable model of signal level statitics on a given path would:

(1) postulate a small number of atmospheric conditions including "normal" atmosphere and atmospheres containing ducts of various characteristics

(2) calculate statistics of signal levels for each of these atmospheric conditions

(3) mix these "modes of propagation" according to the frequency of occurrence of each of them in the region involved.

13

To support such a model it might be sufficient to know simply the frequency of occurrence of surface-based ducts and the frequency of occurrence of elevated layers, this latter to be supplemented with a probability distribution of layer elevations.

3. THE MEASUREMENT PROGRAM

Accompanying our attempts to model signal variability in a ducting environment is a measurement program that uses specially constructed receiving systems to measure and record signal levels from "signals of opportunity." These systems were put into service in the San Diego area in September 1981. The transmitters to which they were tuned were mostly television transmitters in the Los Angeles area about 180 km to the northwest. The systems remained there until August or November 1983, thus giving us what appears to be about 2 years of data. Unfortunately, there were extensive down times and the resulting records are very spotty.

One of the systems was subsequently taken to Boulder, Colorado, and put into service in February 1984. It has since been recording data from a single television station in Pueblo, Colorado, about 190 km to the south.

We want here to describe the equipment used, the propagation paths for which signal levels were measured, and some first-order statistics that were obtained.

3.1 Automated Propagation Measurement System
Equipment Description

The automated propagation measurement system is a special-purpose, microprocessor-controlled receiver. Its function is to receive and record the levels of up to 10 signals in the VHF and UHF ranges for long periods of time. The system tries to fill the need to be able to collect long-term radio propagation data while demanding only a small amount of routine maintenance. The system includes the important features of self-calibration under full control of the microprocessor and self-restart following a power failure.

Near the end of each hour the system will print a summary of the data collected during that hour. The summary gives a number of points on the received signal level distribution for each of the programmed frequencies. In addition to these statistical data some selected values from the calibration process for the current hour are printed. Finally, all of the signal level data collected during the hour, all of the calibration information, and some necessary bookkeeping data are written onto magnetic tape. The routine manual

maintenance, therefore, involves changing the computer terminal paper and the magnetic tape.

The measurement system is composed of two major subsystems--the receiver and the microprocessor. The receiver subsystem, shown in block diagram format in Figure 6, includes components such as the antennas, the antenna control box, the local oscillator (a commercial frequency synthesizer), and the receiver chassis itself (a five-plug-in module device). The microprocessor subsystem is physically divided into several components including the digital tape deck, the computer terminal (keyboard and printer), and the microprocessor chassis. There is one more component of the microprocessor subsystem, and it is probably the most important component of the entire system--the software programs. These not only control all of the functions of the system, but also digitize and record the received signal level data.

Signal energy enters the receiver via one of three receiving antennas. These are connected to an antenna calibration box located nearby at the top of an antenna tower. Particular antennas used are chosen and aimed to acquire the signals from the particular desired signals. For the San Diego measurements the most often used was a horizontally polarized log-periodic antenna with a frequency range from 150 to 1000 MHz. Antennas for the remaining two positions varied with the particular receiver site. Two examples are a yagi tuned to 868 MHz, and another yagi tuned to TV channel 3 at 60 MHz. Proper antenna polarization depends, of course, on the source.

During propagation measurements, the antennas are connected through the antenna calibration box directly to the receiver input. During a calibration period, a switch disconnects the antennas and substitutes a broadband noise source. This provides a known signal level across all measurement frequencies. Since the noise diode calibration signal passes through exactly the same signal path as the received signal, this technique accurately compensates for all features of the signal path--regardless of the amount of attenuation or gain present in a given channel. The only uncalibrated parts of the signal path are the antennas themselves and the short lead-ins between antennas and calibration box inputs.

Most of the remainder of the receiver is contained in a series of modules that fit into a commercial instrument chassis. The signals first pass through a signal-conditioning module where the desired signals are separated from other frequencies with rf bandpass filters (typically 20 MHz wide) and
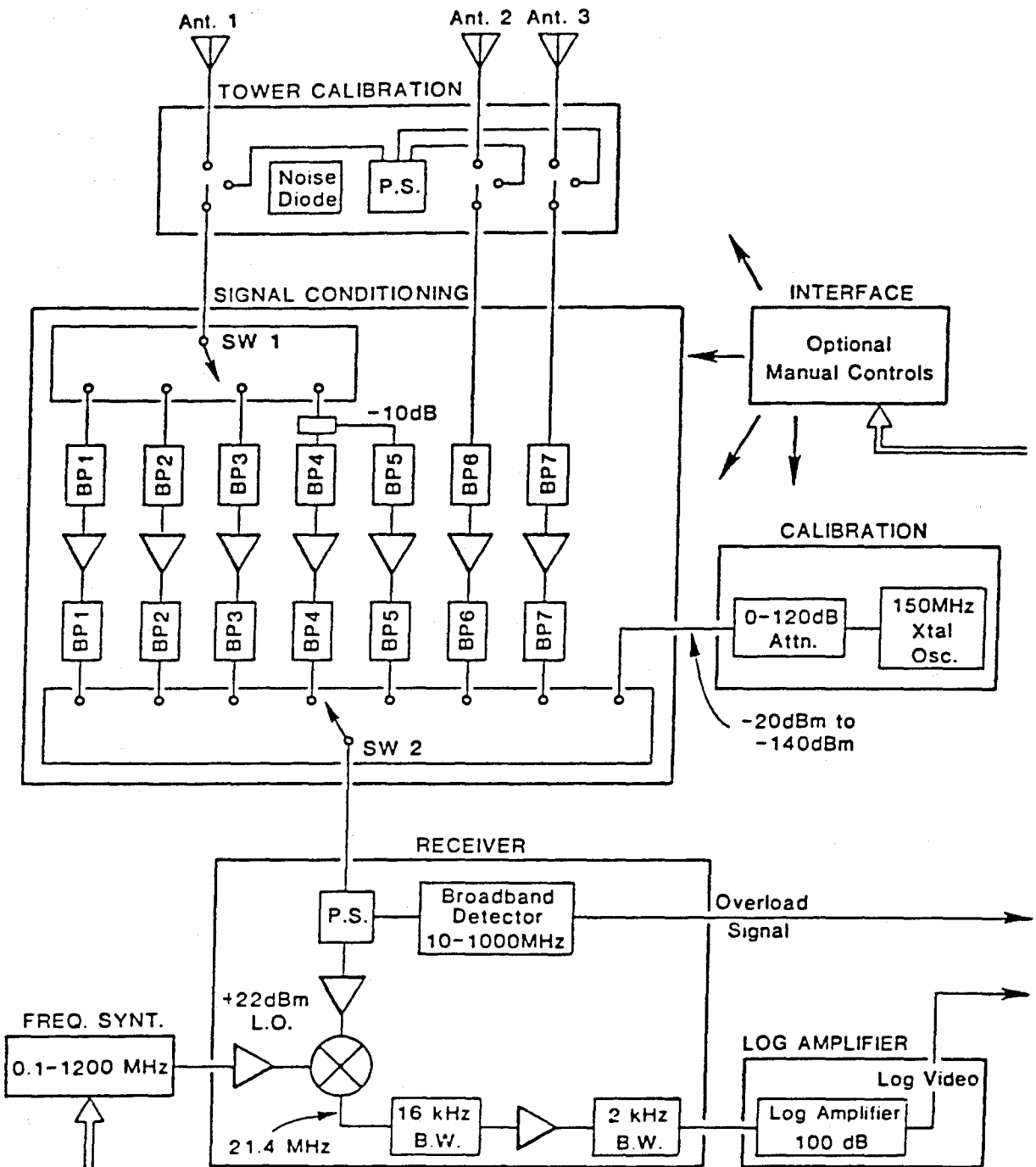
Figure 6. Block diagram for the receiver subsystem of the Automated Propagation Measurement System.

amplified with low-noise preamplifiers. The exact bandpass filters used will vary with the frequencies selected to be received at each site, and therefore the module is constructed so as to allow easy replacement. In Figure 6 the switch SW1 is a very long-life mechanical rf switch that has a high insertion loss and should resist possible intermodulation products from strong out-of-band signals. The rf switch SW2 is a simple PIN-diode switch that can be used here because insertion loss and intermodulation performance have already been assured by the preceding signal conditioning.

The receiver module is a single-conversion, superheterodyne receiver with a 21.4 MHz IF frequency. A final bandpass of 2 kHz provides a measurement noise floor at about -118 dBm. Meaningful output from the system presupposes well-known and stable source transmitter frequencies. Part of the rf signal is split off for a broadband detector. This detector senses the total power in the rf band-pass and indicates a possible overload problem if too much signal power is present. The receiver frequency is precisely selected by the local oscillator frequency, which is provided by a commercial frequency synthesizer. The output of the synthesizer is amplified to +22 dBm for high-level mixing to reduce the susceptibility to intermodulation products.

The IF signal is converted to a DC voltage by the logarithmic amplifier module with a 100 dB dynamic range. Operation over this very large dynamic range assures accurate measurements even if input signal amplitude changes over a very wide range. The logarithmic amplifier module also contains an audio amplifier and a loudspeaker, which may be useful for diagnostic purposes.

The calibration module contains a 150 MHz signal source and a 120 dB step attenuator. These provide a known calibration signal over a -20 to -140 dBm range and will characterize the log amplifier response in 10 dB steps.

The entire receiver can be controlled manually or automatically via a computer program. When the receiver is being used for measurements, it will normally be under computer control. Testing and trouble-shooting are often easier under manual operation. Many of the manual controls are located on the digital interface module. Other controls are positioned on the modules that they control.

The module chassis contains power supplies and interconnection wiring used by the modules. Most of the IF and rf signal paths go through coaxial

17

cabling on the front panels of the modules, because the connectors on the back of the modules are not designed to handle radio frequencies.

A high-accuracy frequency synthesizer is the last major subassembly of the measurement system. This instrument generates the required local oscillator (LO) frequencies, as commanded by the computer via an IEEE-488 data bus. The synthesizer is a standard instrument, although an internal jumper has been positioned to speed up tuning and accuracy at the expense of some (unused) modulation capability.

A microprocessor-based control and analysis system operates the receiver. Under the control of measurement programs stored in ROM (Read Only Memory) and magnetic bubble memory, the receiver is cycled through a preestablished sequence of measurement frequencies, using proper antennas and signal-conditioning paths. At the beginning of each hour a complete system recalibration is accomplished with a combination of calibration techniques involving the noise diodes and the 150 MHz calibration oscillator. These frequent calibrations should keep the signal level measurements accurate in the face of possible system gain drift.

Laboratory testing of the receiver system with known signal inputs indicates that the recorded signal level can be up to 4 dB away from the signal level injected at the antenna calibration box. The magnitude of error is more pronounced when low-level signals are being monitored. For example, the widest discrepancy between actual signal level and recorded signal level occurred in a test at 687.24 MHz. A -90 dBm signal was injected at the antenna calibration unit, and statistics of its measured level were recorded in the automatic measurement mode over a standard 50-min test cycle. While the record showed a signal level greater than -90 dBm for more than 99% of the time, it also indicated a level greater than -86 dBm for 5% of the time. Hence, one should keep in mind that some degree of error, perhaps up to as much as 4 dB, may be associated with much of the automated propagation measurement system data.

3.2 Paths

There were somewhat more than 30 paths whose signals were used for this program. Of these we would like to describe here 14 that are interesting for our purposes and for which we seem to have a useful number of valid data.

The three San Diego receiver sites were located in three rather different local environments. The first was at the FCC Field Office located in a five-

18

story building in La Mesa, a suburb on the northern edge of San Diego. The second was part of a small antenna farm on Cowles Mountain, a small mountain (477 m high) northeast of La Mesa. And the last receiver site was on Point Loma, a United States naval reservation on the Pacific Ocean at the northwestern corner of San Diego.

The transmitters were all "signals of opportunity" derived from television stations. Now, the use of television transmitters as signals for propagation studies has its advantages and its disadvantages. Among the advantages are high radiated power, very good frequency stability, and a sharply localized spectrum. A UHF television station will often have an effective radiated power (ERP) of as much as 5 MW and almost all of this power will be localized in the video carrier. There are, however, at least two disadvantages. First, a station is not normally in operation for the full 24 hours of the day and there will be regular gaps in the record. Indeed, operating hours for some of the stations observed in the present program were rather short. The second concern is with the antenna patterns. These may be omnidirectional in that they radiate equally in all azimuthal directions, but they are almost always high gain antennas with a sharp beam in the vertical plane. Beam widths can be 2° or even less. If an antenna is on a mountain overlooking the area to be served, it will often employ electrical beam tilting and direct the beam downward by 1° or 2° toward the desired service area. Since we are interested here in interference fields where elevation angles to shielding terrain obstacles may be out of the ordinary and where a layered atmosphere may bend the rays in unusual directions, it is therefore difficult to say how one should treat these narrow beams. In particular, it seems questionable whether one can immediately transfer results obtained by a study of such television transmitters to the case of the mobile services where lower gain antennas are normally used.

The paths extend along the California coast between Los Angeles and San Diego, and they are subjected to a radio climate dominated by what is called the "marine layer." This is a layer of marine air trapped by a temperature inversion that extends along the coast and out into the Pacific Ocean. Its depth undergoes considerable variabiliy with an average near Los Angeles of about 500 m. Accompanying it there often appear one or more super-refractive layers that may then affect radio waves. Winter storms, of course, will blow away the marine layer leaving only a "normal" atmosphere.

3.2.1 KEYT(3), Santa Barbara

Although the principal purpose of the program was to measure UHF signals, we did observe a few VHF stations. One of them, KEYT(3), operates at the particularly low frequency of 61 MHz. It was made part of the program because of a particular need of the FCC to study the effects a proposed San Diego based Channel 3 station would have on the environment.

The station is network affiliated, radiates maximum permitted power, and normally operates from 0600 to 0100 local time. It serves Santa Barbara and the adjacent coastal cities some 140 km northwest of Los Angeles. The antenna is on TV Peak in the Santa Ynez Mountains at an altitude of 1324 m. It should be above the marine layer most of the time.

The station was received at both Cowles Mountain and Point Loma. In Figures 7 and 8 we show the terrain profiles of the two paths. Note that they can both be characterized as long (330 km) oversea paths with horizons on the water.

3.2.2 KABC(7), KWHY(22), and KLCS(58); Mt. Wilson

These three television transmitters are all located in the antenna farm on Mt. Wilson northeast of Los Angeles. Their widely separated carrier frequencies should provide us the opportunity to describe directly how received signal levels vary with frequency.

KABC (175 MHz) is network affiliated, transmitting maximum permitted power. It is another of the VHF stations observed. Its normal operating hours are from 0530 to 0330, and this station is the most nearly continually operating of all the broadcast stations observed. It was received at all three San Diego sites.

KWHY (519 MHz) is an independent station that operates as a subscription television station using a scrambled signal in the evenings. It transmits maximum permitted power and normally operates between the hours 0630 and 2430. It was received at both La Mesa and Cowles Mountain.

KLCS (735 MHz) is a public television station operated by the Los Angeles Unified School District. It transmits at nearly the maximum permitted power; unfortunately, its operating hours are rather short, from 0730 to 2130 and even less on the weekends. It was received at all three receiver sites.

The three antenna towers are all very close together almost 1800 m above sea level. The eight paths involved (examples of which are shown in Figures 9, 10, and 11) are all very similar. They are about 185 km long, but because
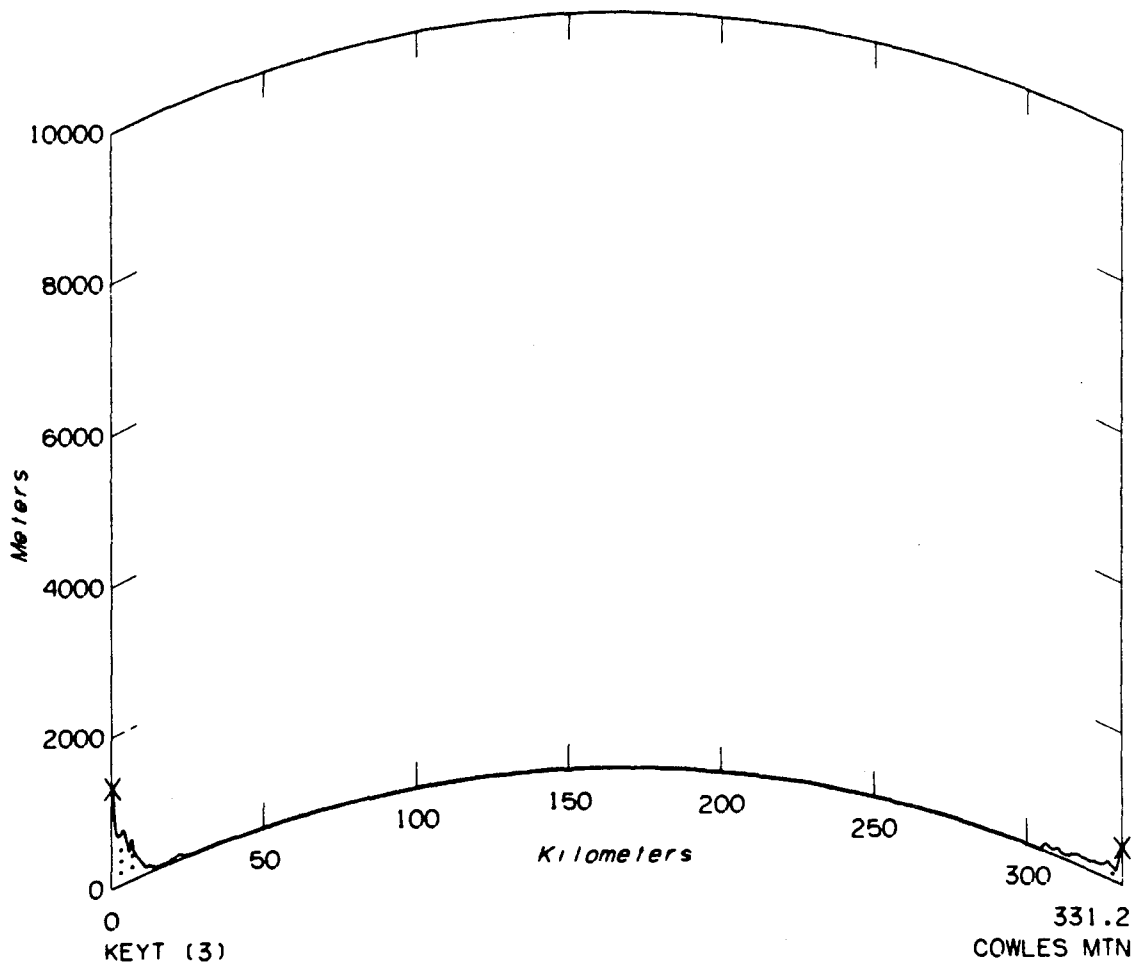
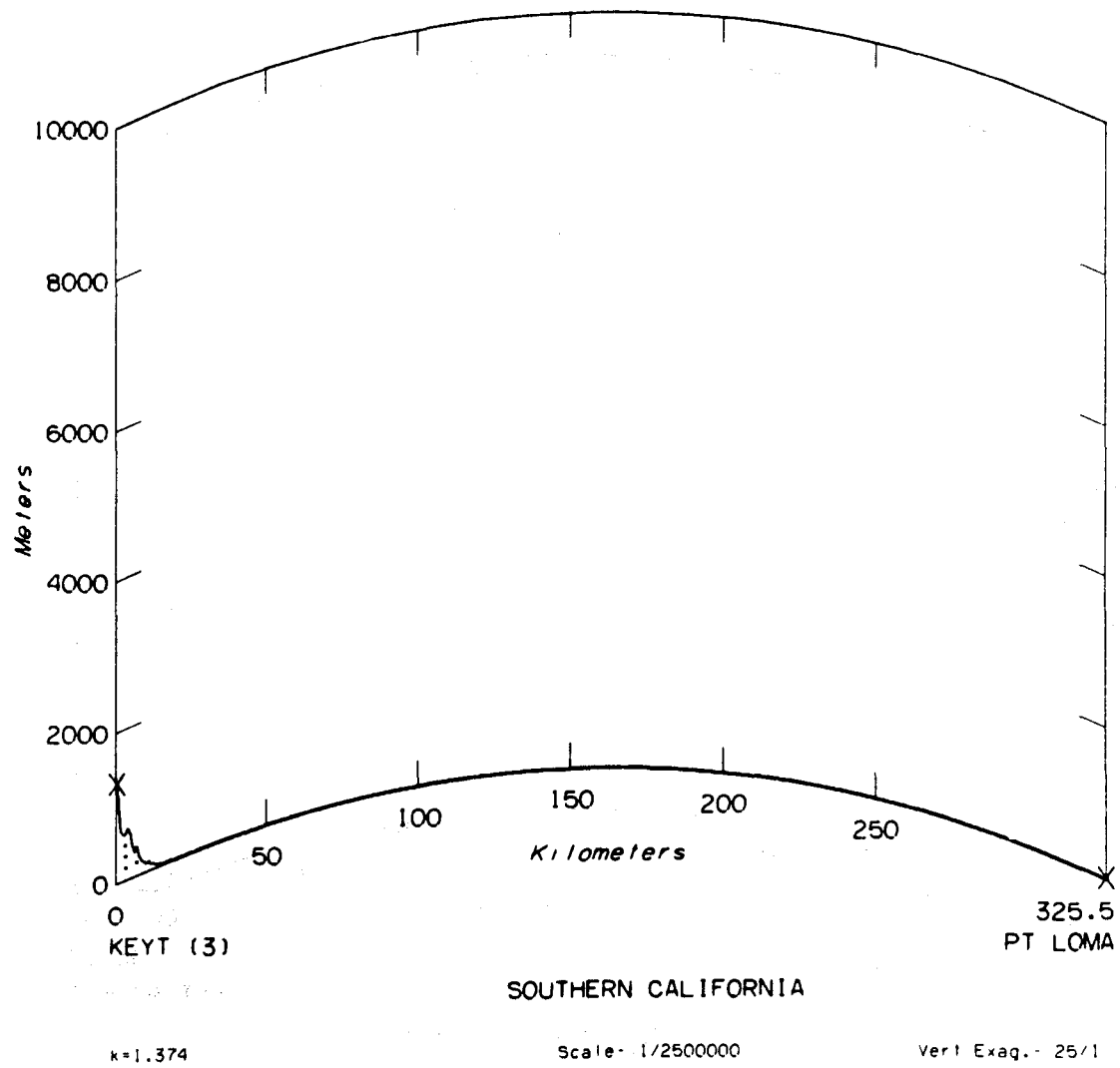Figure 7. Terrain profile: KEYT(3) to Cowles Mountain.

Figure 8. Terrain profile: KEYT(3) to Point Loma.

22
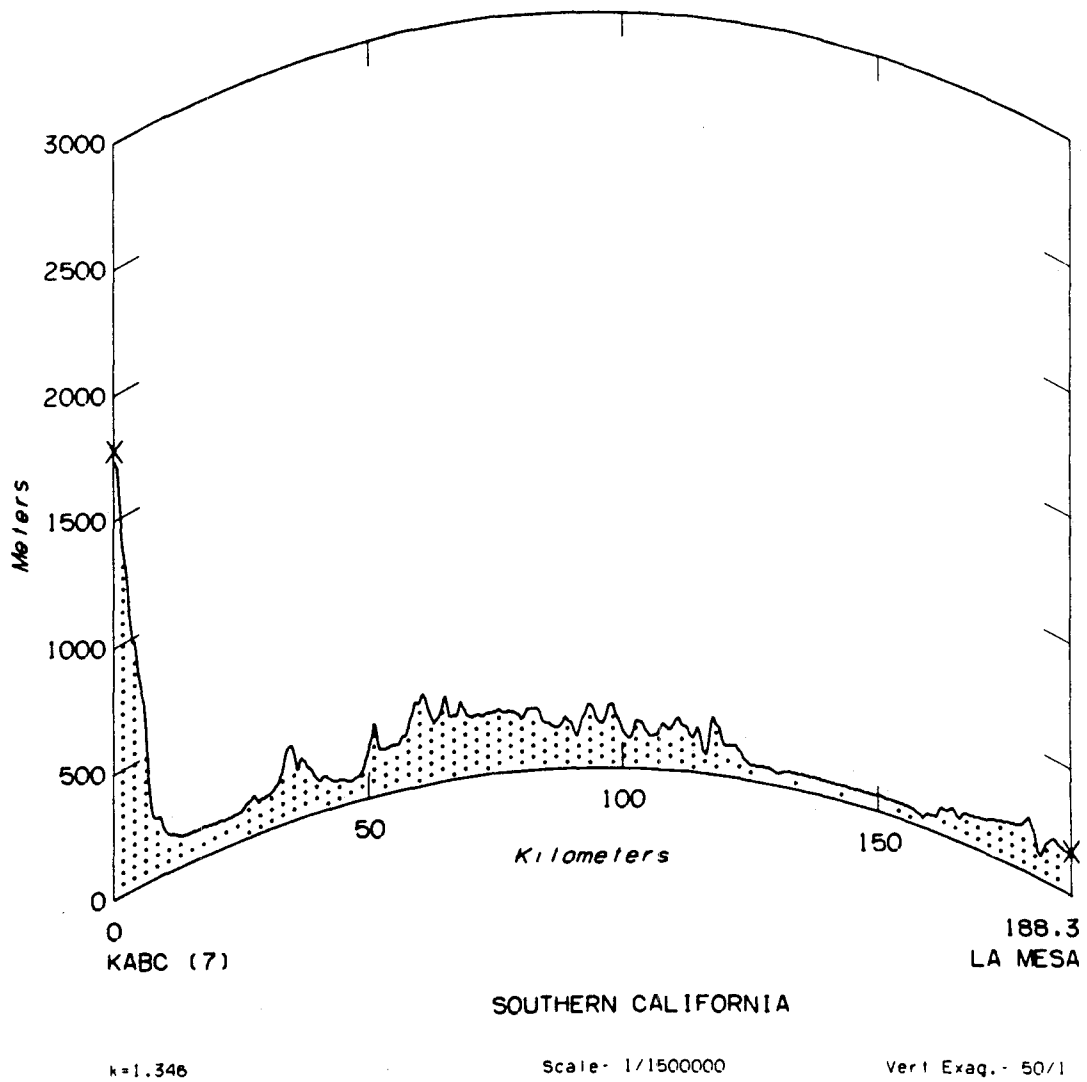
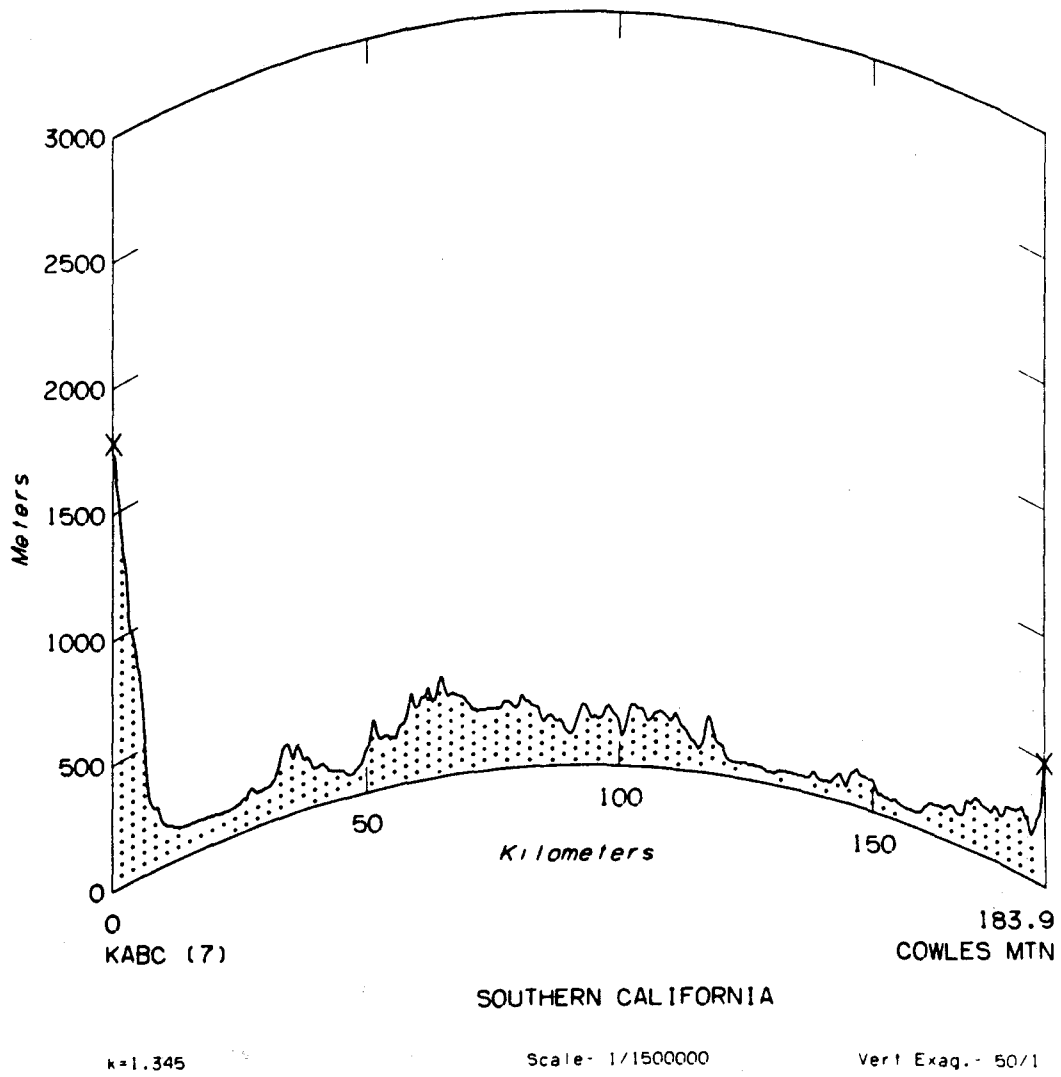Figure 9. Terrain profile: KABC(7, Mt. Wilson) to La Mesa.

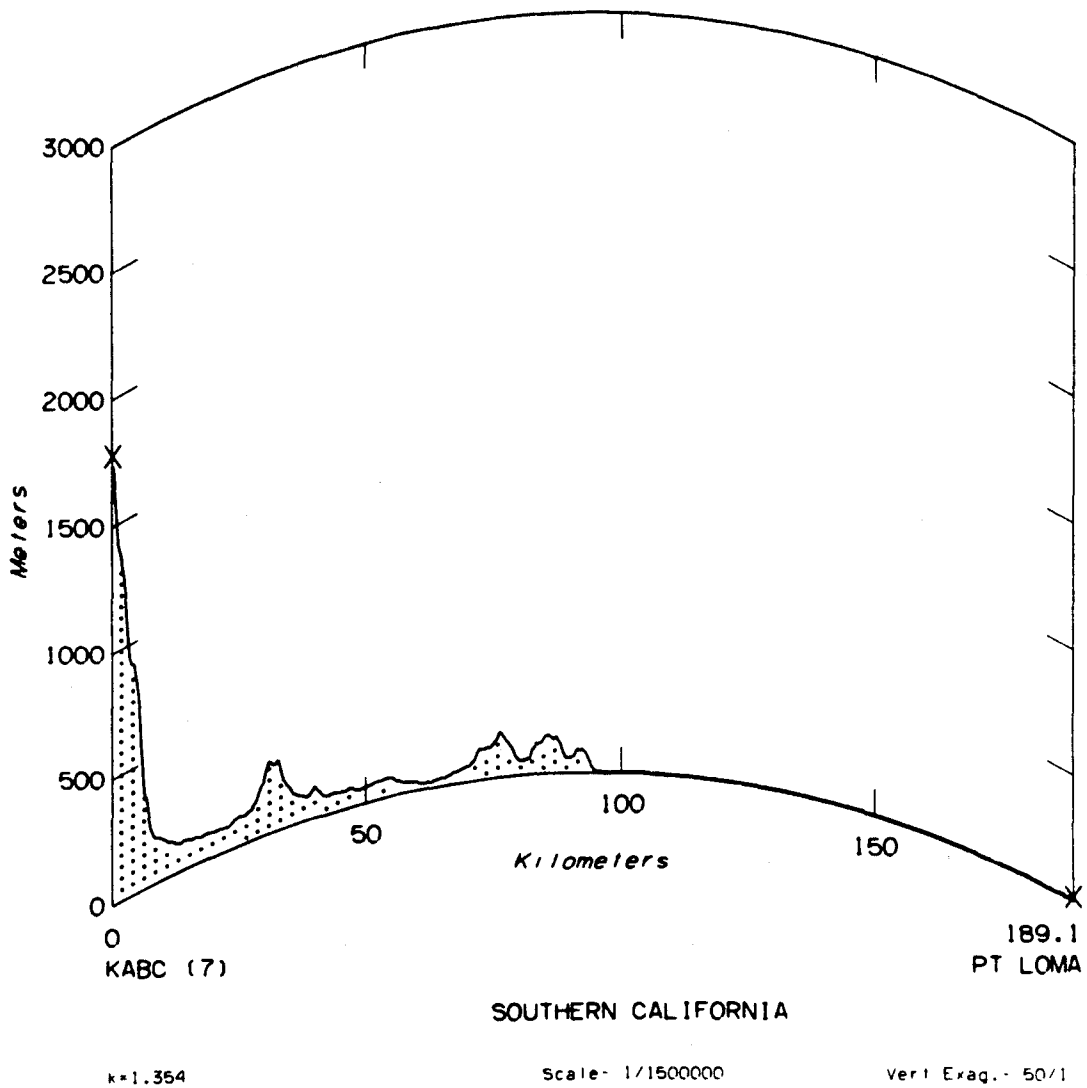Figure 10. Terrain profile: KABC(7, Mt. Wilson) to Cowles Mountain.

3000

2500

2000

Meters

1500

1000

500

0

0
KABC (7)

50

Kilometers

100

150

189.1
PT LOMA

SOUTHERN CALIFORNIA

k=1.354

Scale- 1/1500000

Vert Exag.- 50/1

Figure 11.   Terrain profile: KABC(7, Mt. Wilson) to Point Loma.

of the high transmitters they are all line-of-sight or nearly line-of-sight
paths. The paths to Cowles Mountain are, indeed, line-of-sight. Those to
La Mesa are interrupted by a mountain ridge about 9 km in front of the
receiver, and those to Point Loma by a local hill only 0.6 km in front of the
receiver. Note that if we postulate a marine layer 500 m high, then rays
emerging from the transmitter will be tangent to that layer at a distance of
about 145 km. This would be from 40 to 50 km in front of the receiving
terminals.

3.2.3 KOCE(50), La Habra

KOCE(50) is a public television station operating at 687 MHz and with
maximum permitted power. Its normal operating hours are from 0530 to 2400.
Although it serves Huntington Beach, its transmitter is about 30 km away in
the Puente Hills overlooking La Habra. These locations are in the southern
part of the Los Angeles area and, indeed, the station probably reaches most of
the communities there. The antenna is 469 m above sea level which is well
within the range of elevations assumed by the top of the marine layer.
Although somewhat inland, the antenna should be above the marine layer some of
the time and within it at other times.

The station was observed at all three receiver sites and the resulting
path profiles are shown in Figures 12 to 14. The paths are long (about
155 km) and are interrupted by some low mountains at about midpath. The path
to Point Loma is largely over the sea, but the two horizons are both on land,
the one near the receiver being a local hill only 0.5 km away. The three
paths show quite a number of differences, and this, coupled with the behavior
of the marine layer, should make the results very interesting.

3.2.4. KTCS(8, Pueblo) to Boulder, Colorado

This is the path that resulted when one of the receiver systems was moved
to Colorado. The radio climate in this new location is greatly different. In
Colorado the air is thin and dry and super-refractive layers are a rarity.

The receiver was in an ITS laboratory in a one-story wing of a building
near the southern edge of Boulder. The transmitter is a VHF television
station (181 MHz) operating at maximum permitted power. It is a public
television station with normal operating hours from 0600 to 2300.
Unfortunately, in the summer it goes to a reduced schedule and is on the air
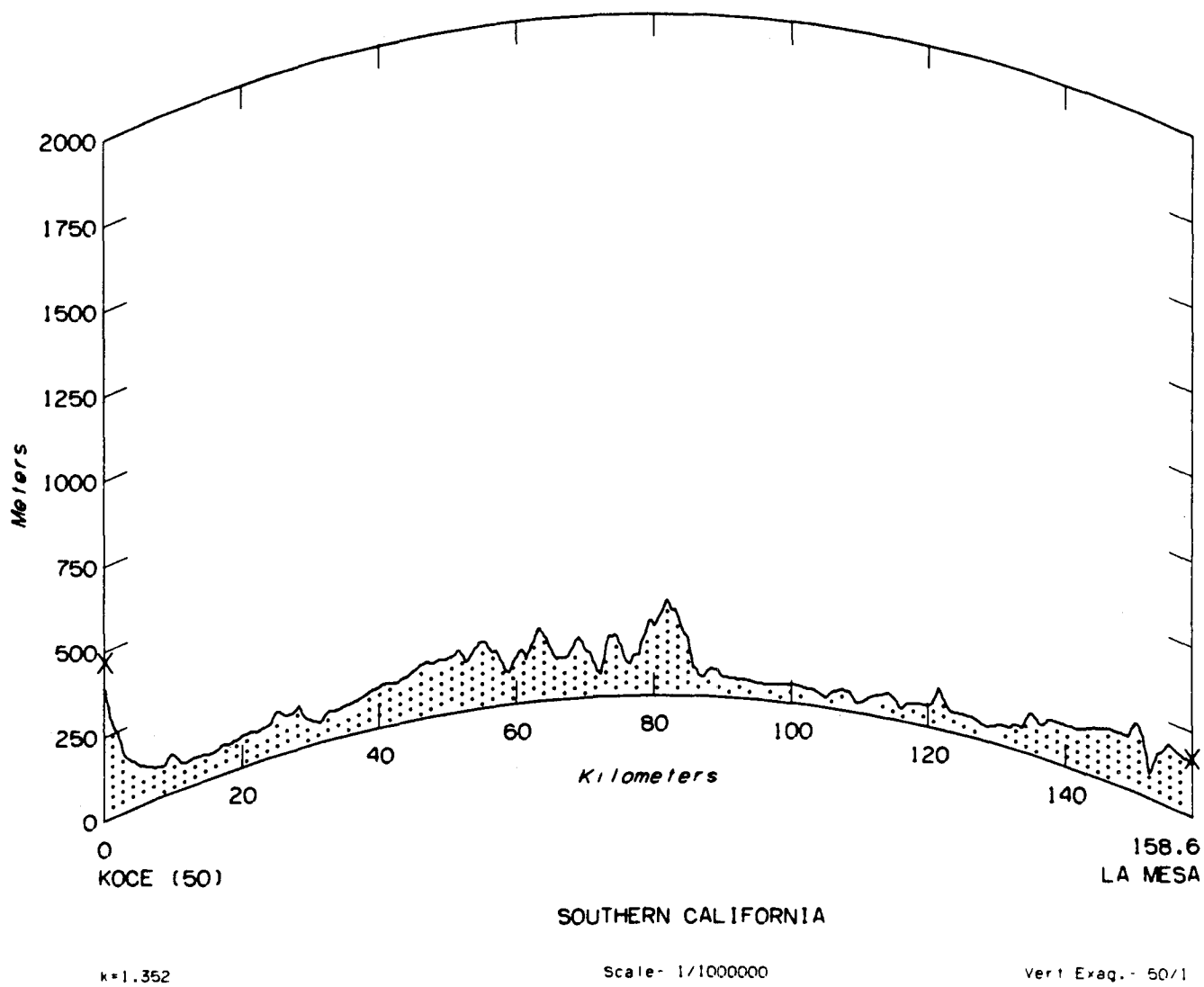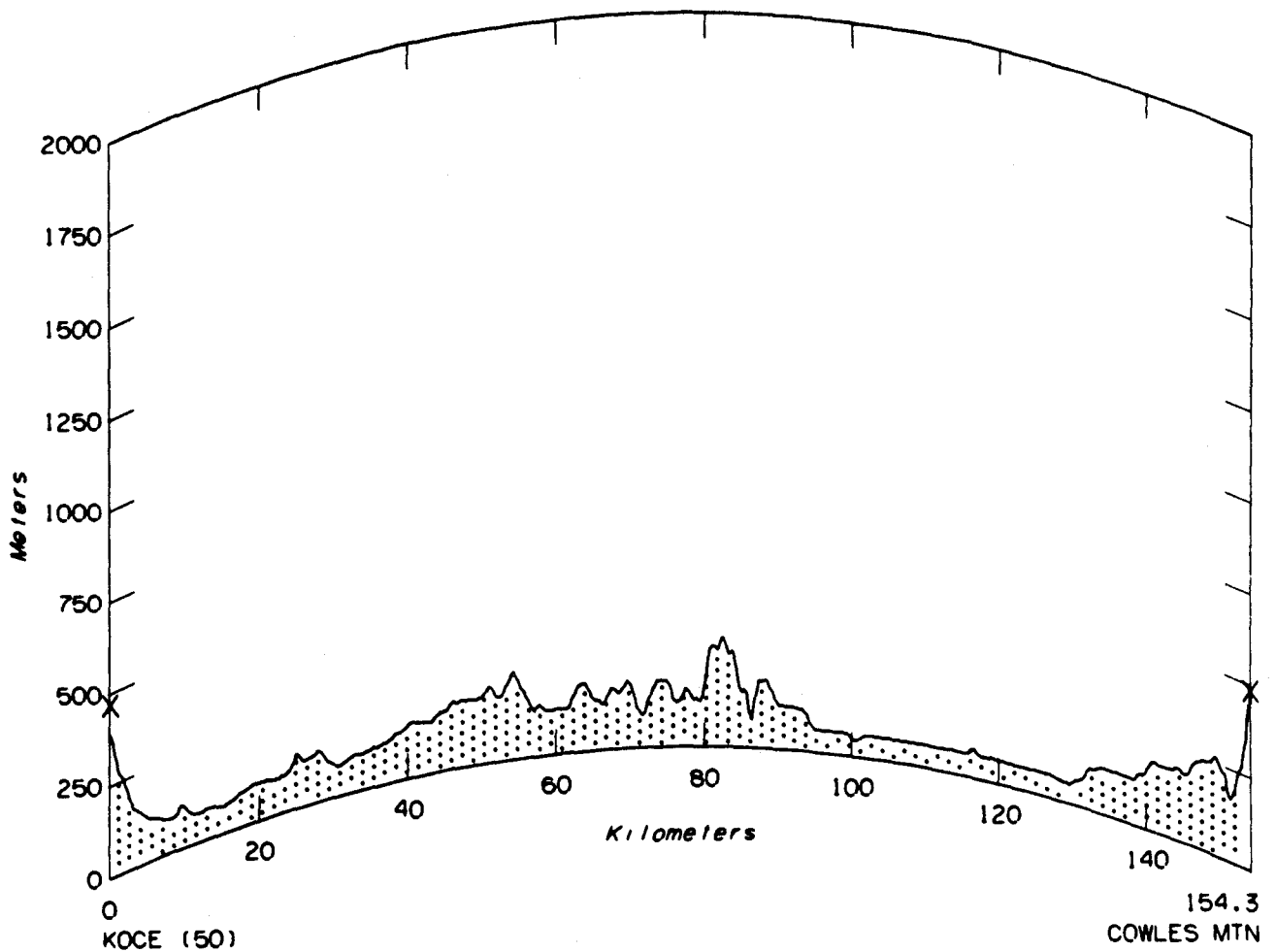only from 1400 to 2300.

Figure 12. Terrain profile: KOCE(50) to La Mesa.

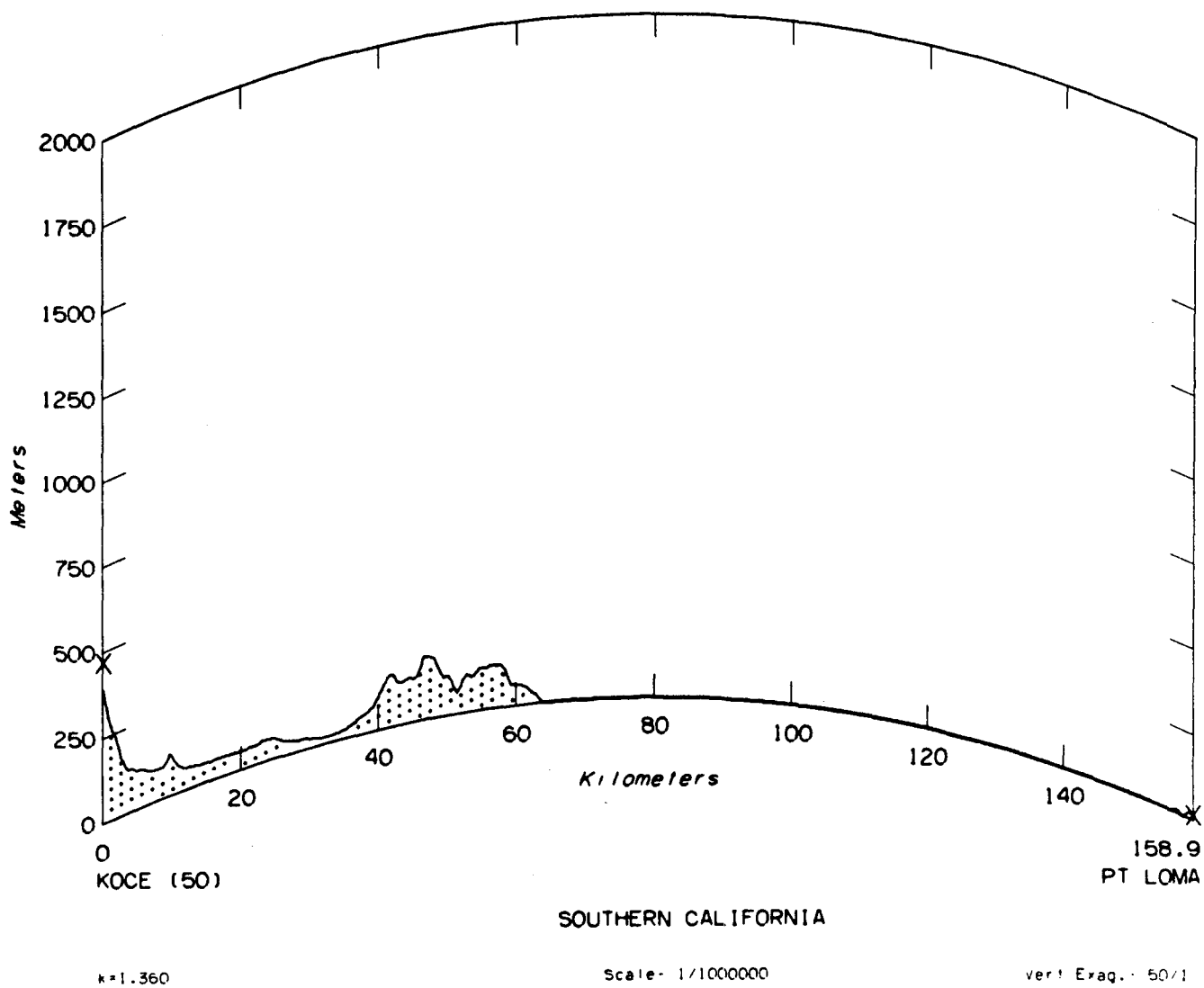Figure 13. Terrain profile: KOCE(50) to Cowles Mountain.

Figure 14. Terrain profile: KOCE(50) to Point Loma.

The terrain profile is shown in Figure 15. The path runs through the plains of eastern Colorado parallel to, but not far removed from, the Rocky Mountains. The peak in the middle of the path is one of the foothills that happens to intrude. The actual horizon for the receiver is a small hill about 9 km away.

3.3. First-Order Results

With the kind of measurements being obtained we would suppose that there are many sorts of analyses that might be usefully developed. As we pointed out before, however, the data are very spotty and of mixed quality so that analyses are difficult to make and when made they would be difficult to interpret. For example, the two seasonal extremes, in February and August, seem greatly underrepresented in the data and whether one should (or even could) make suitable allowances requires consideration.

We have chosen here to make only a simple first-order analysis in which we have lumped together into an individual statistical ensemble all available data for each path. In Figures 16 through 29 we have plotted the resulting cumulative distributions of the hourly medians of attenuation relative to free space. Included on those graphs are predictions given by the two methods described in Section 2.2. We have called them, but only for convenience, the ITM (as demonstrated in Figure 5) and the CCIR methods. Note that the latter tries to predict only for 1% or less of the time, and that is why it appears as a short segment on the left side of a graph.

Some of the predictions given here, such as the two in Figure 24, are remarkably accurate; some, such as those in Figure 27, are so-so; but many are very different from the measured data. We have, of course, the problem of spotty data and the uneven representation of diurnal and seasonal periods, and perhaps a more consistent and extensive set of data would have produced quite different measured curves. But more generally, we should not be surprised that prediction and data differ, for the environment here is far different from the "normal" environment envisaged by the models and, especially, the path parameters used here are often outside the professed ranges. For example, the CCIR method has been developed only for fairly high frequencies, and while we have therefore not attempted to use this method for the TV Channel 3 data in Figures 16 and 17, we have, to the contrary, struggled to extrapolate the curves back to frequencies for Channels 7 and 8.
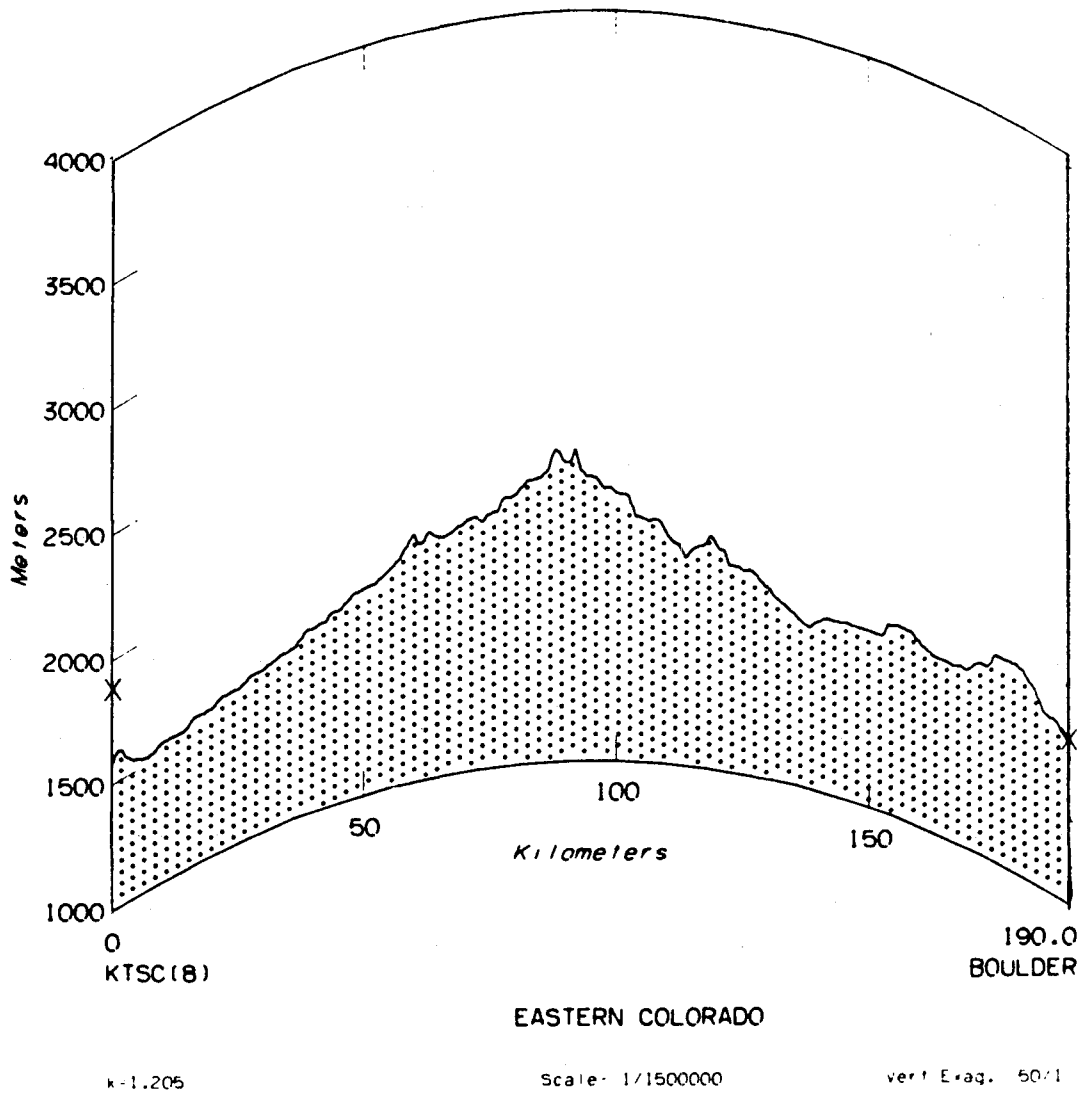
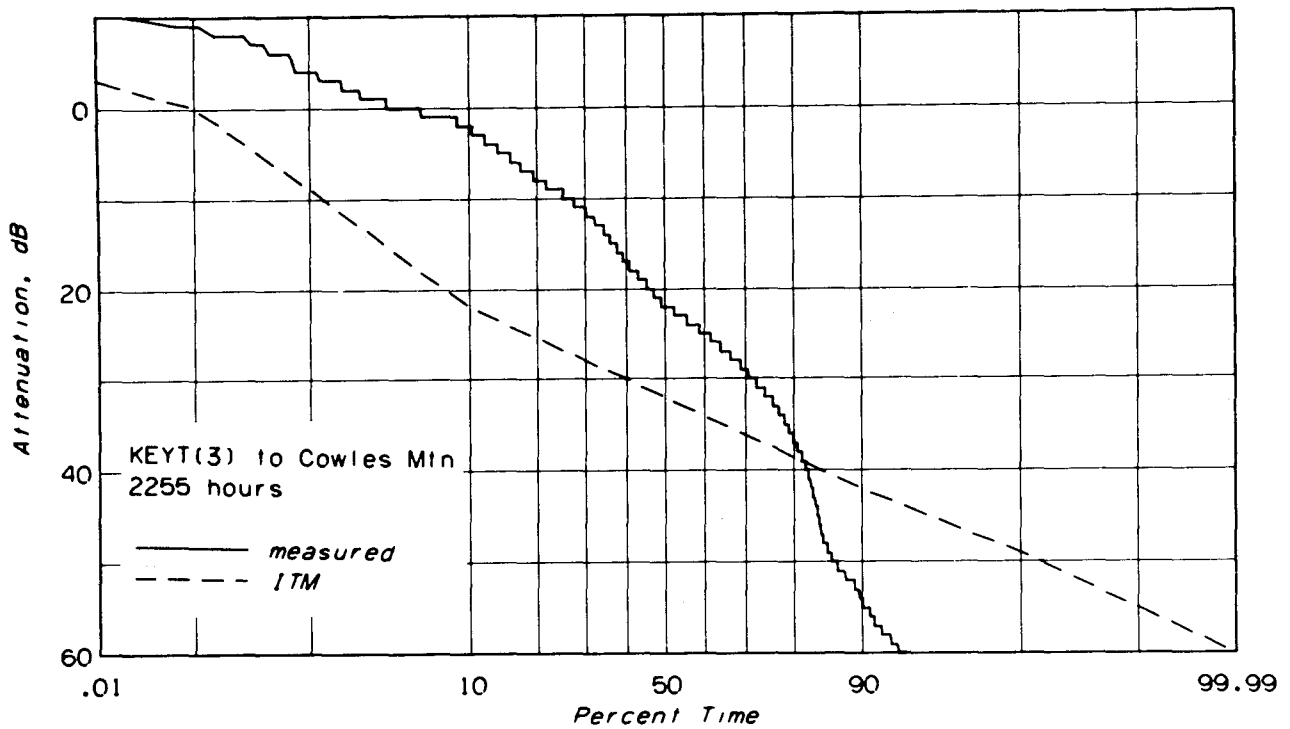Figure 15. Terrain profile: KTSC(8) to Boulder.

Figure 16. Cumulative distribution of the hourly median data obtained on the path from KEYT(3) to Cowles Mountain.
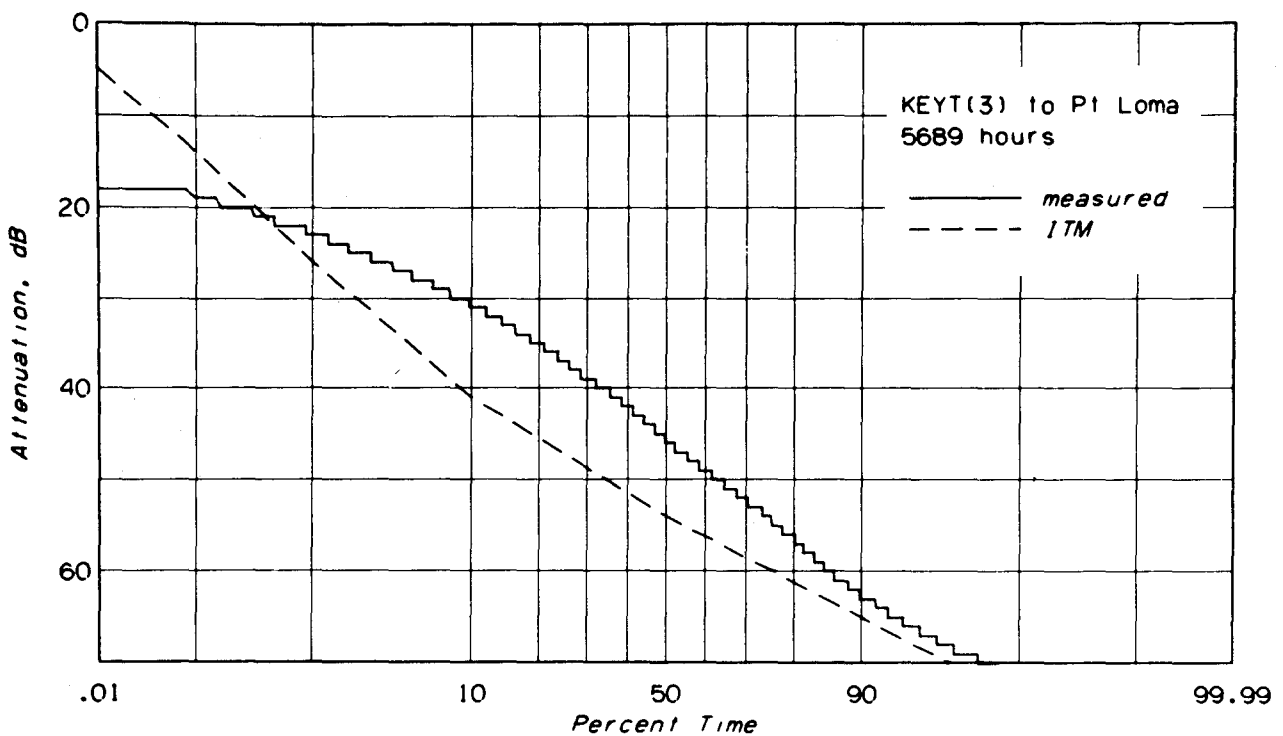

Figure 17. Cumulative distribution of the hourly median data obtained on the path from KEYT(3) to Point Loma.
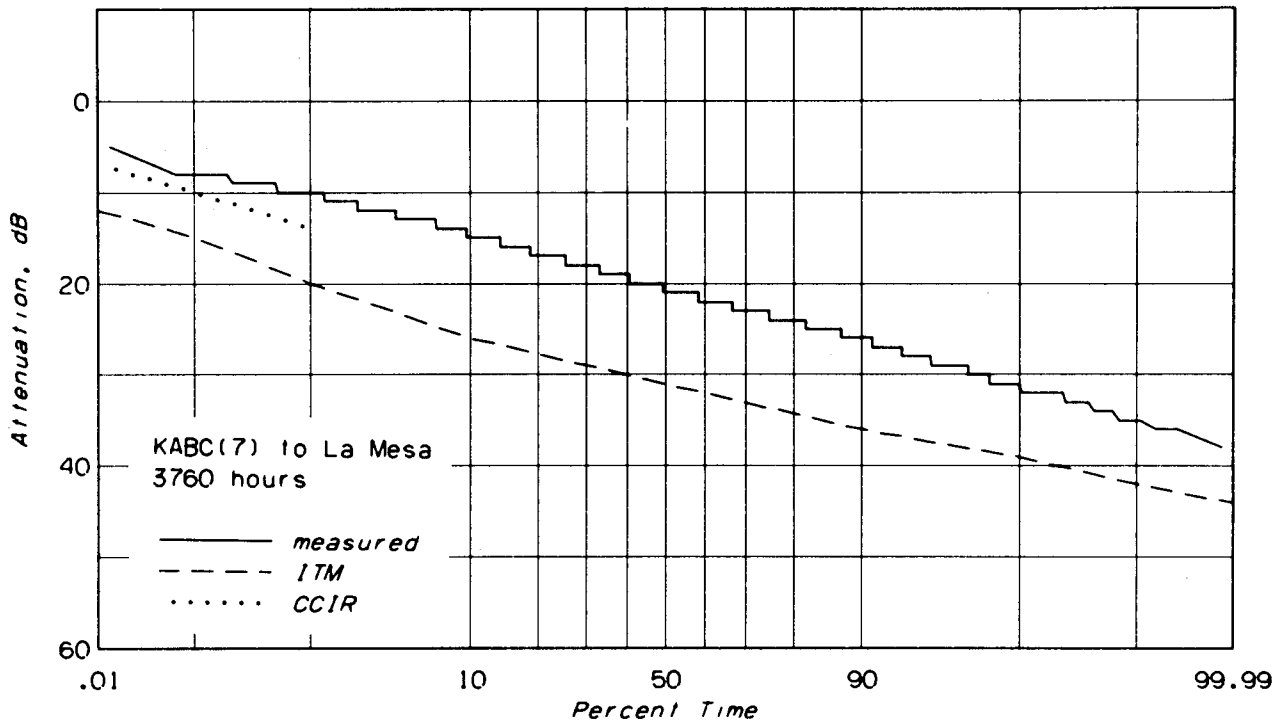
Figure 18. Cumulative distribution of the hourly median data obtained on the path from KABC(7) to La Mesa.
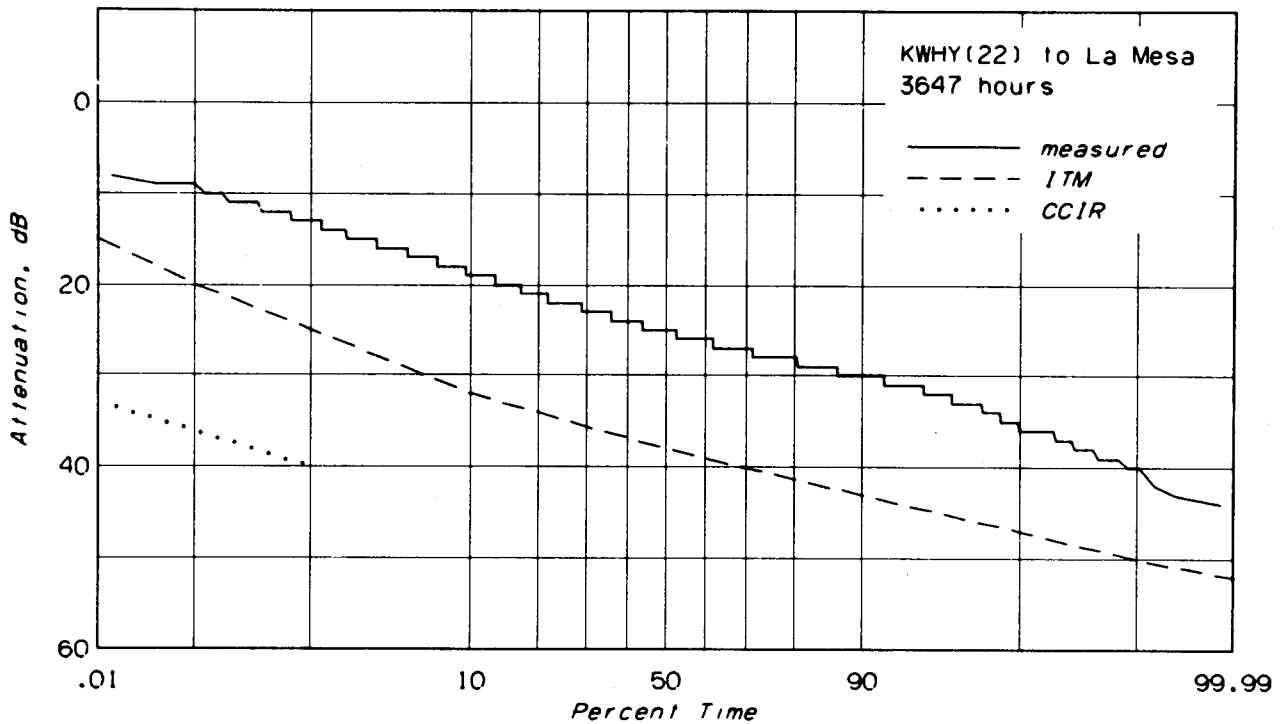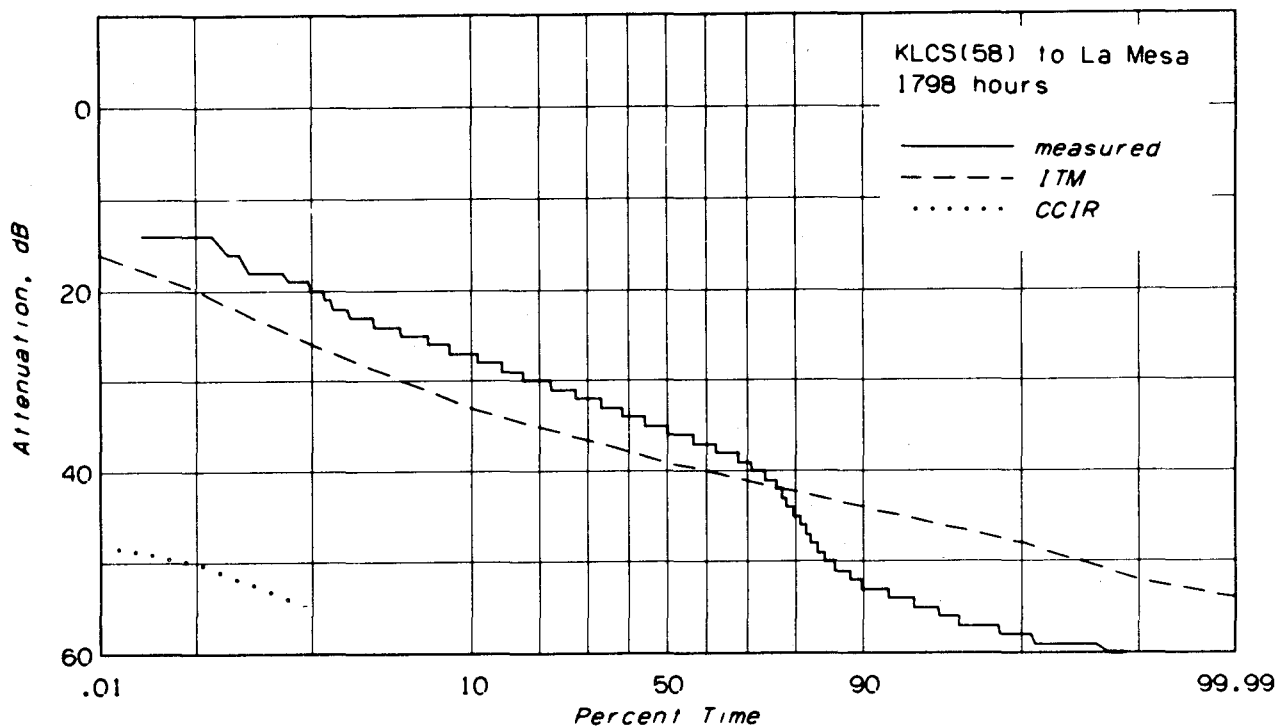

Figure 19. Cumulative distribution of the hourly median data obtained on the path from KWHY(22) to La Mesa.

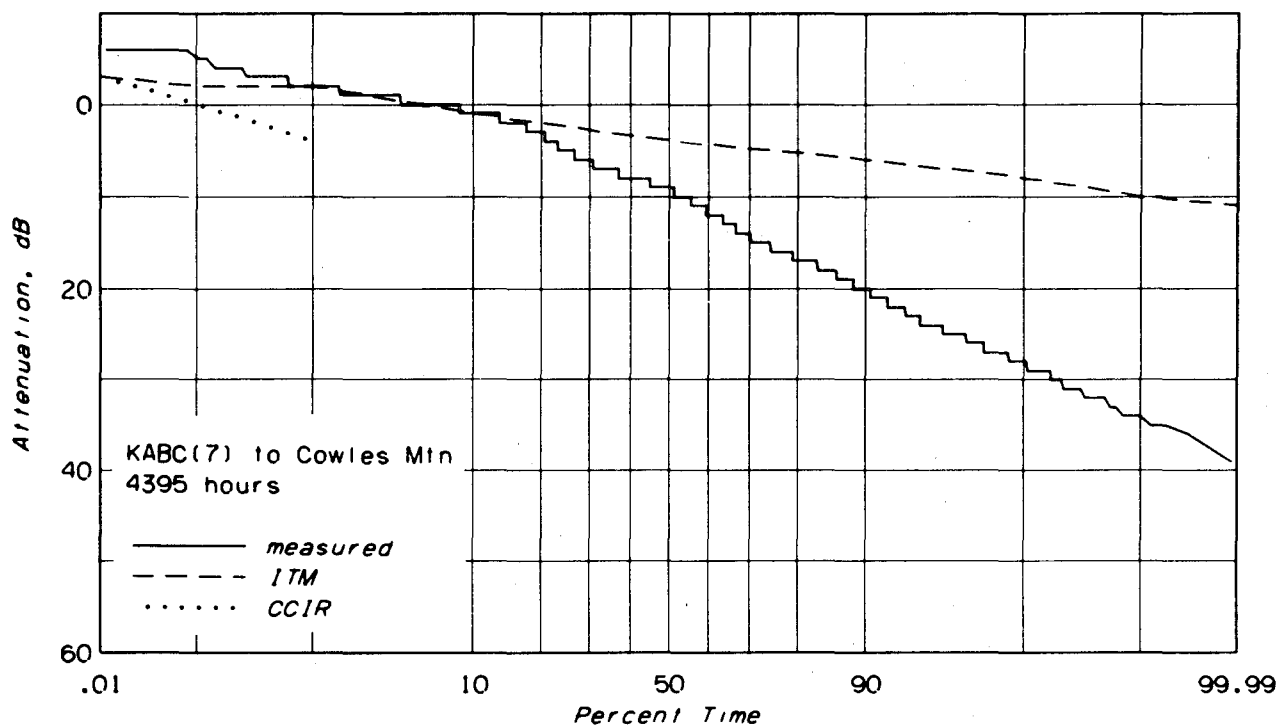Figure 20. Cumulative distribution of the hourly median data obtained on the path from KLCS(58) to La Mesa.

Figure 21. Cumulative distribution of the hourly median data obtained on the path from KABC(7) to Cowles Mountain.
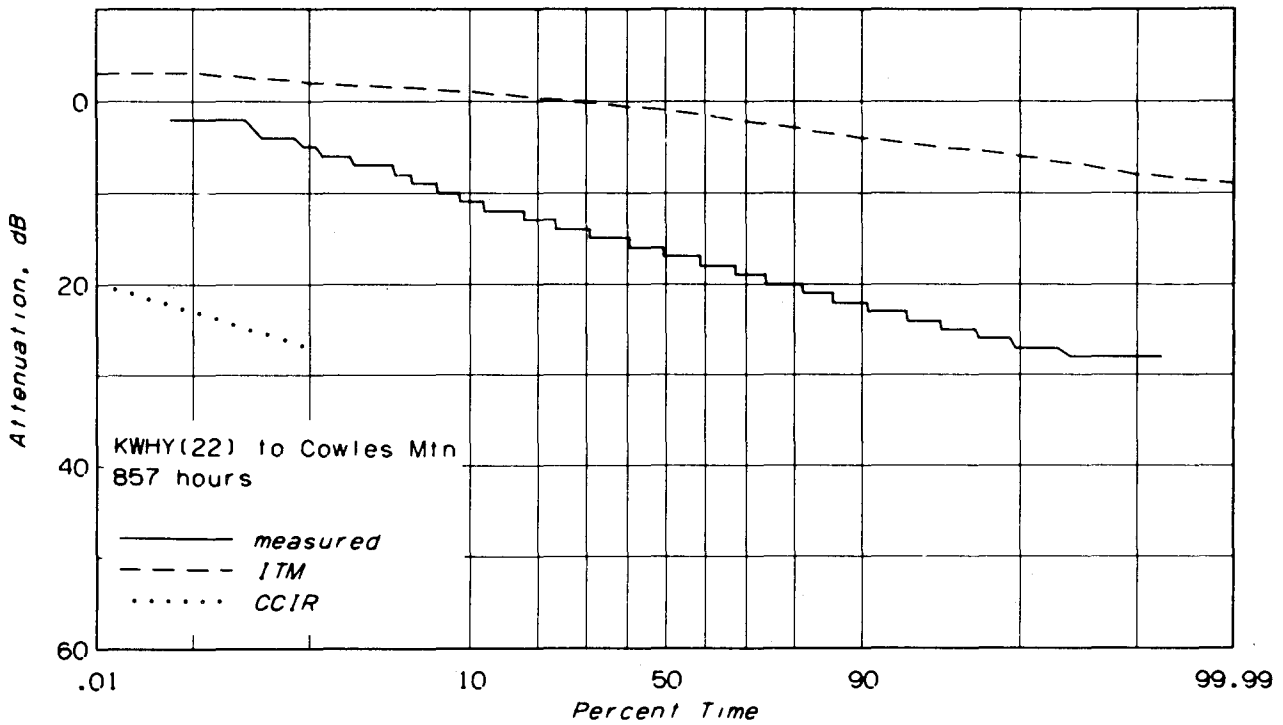
Figure 22. Cumulative distribution of the hourly median data obtained
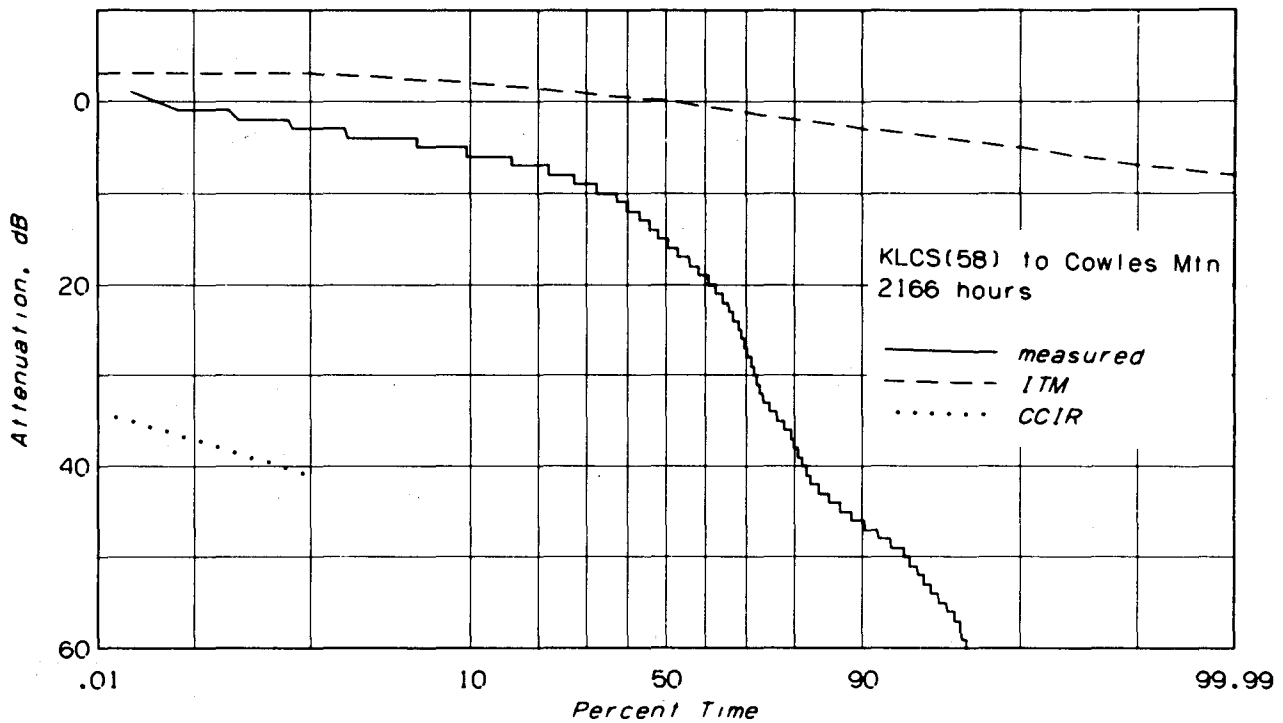on the path from KWHY(22) to Cowles Mountain.

Figure 23. Cumulative distribution of the hourly median data obtained
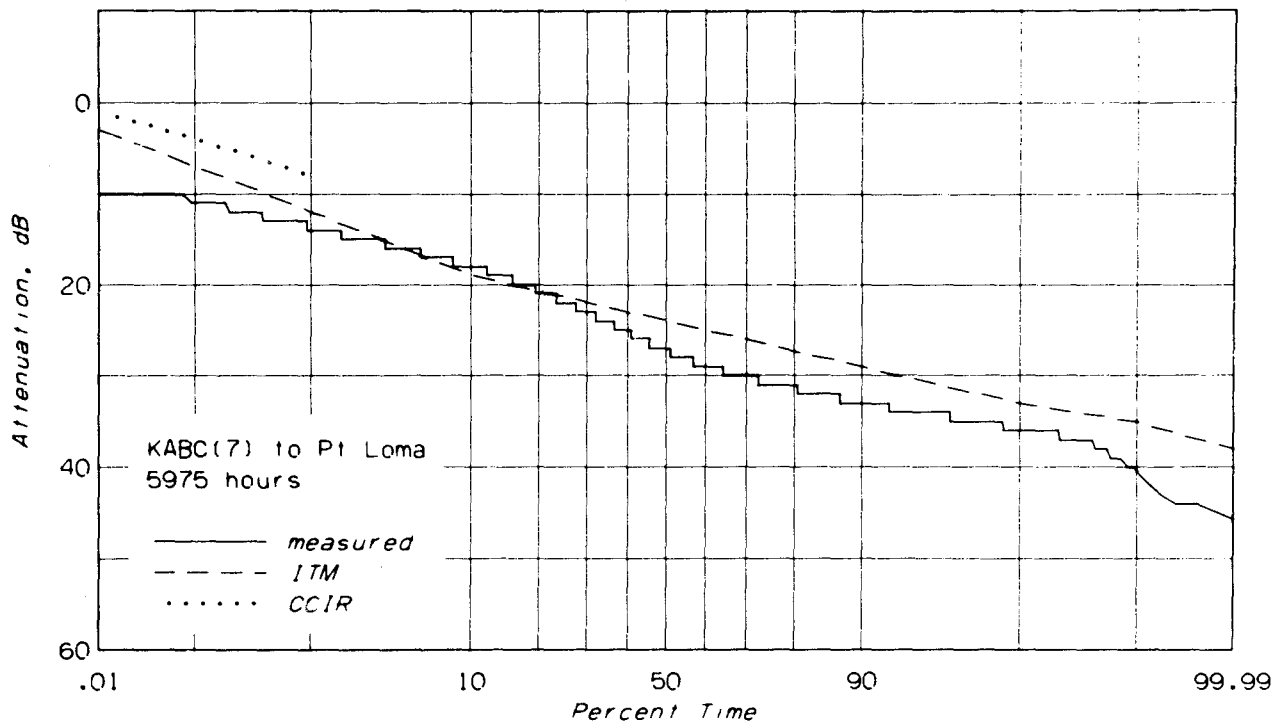on the path from KLCS(58) to Cowles Mountain.

35

Figure 24.   Cumulative distribution of the hourly median data obtained
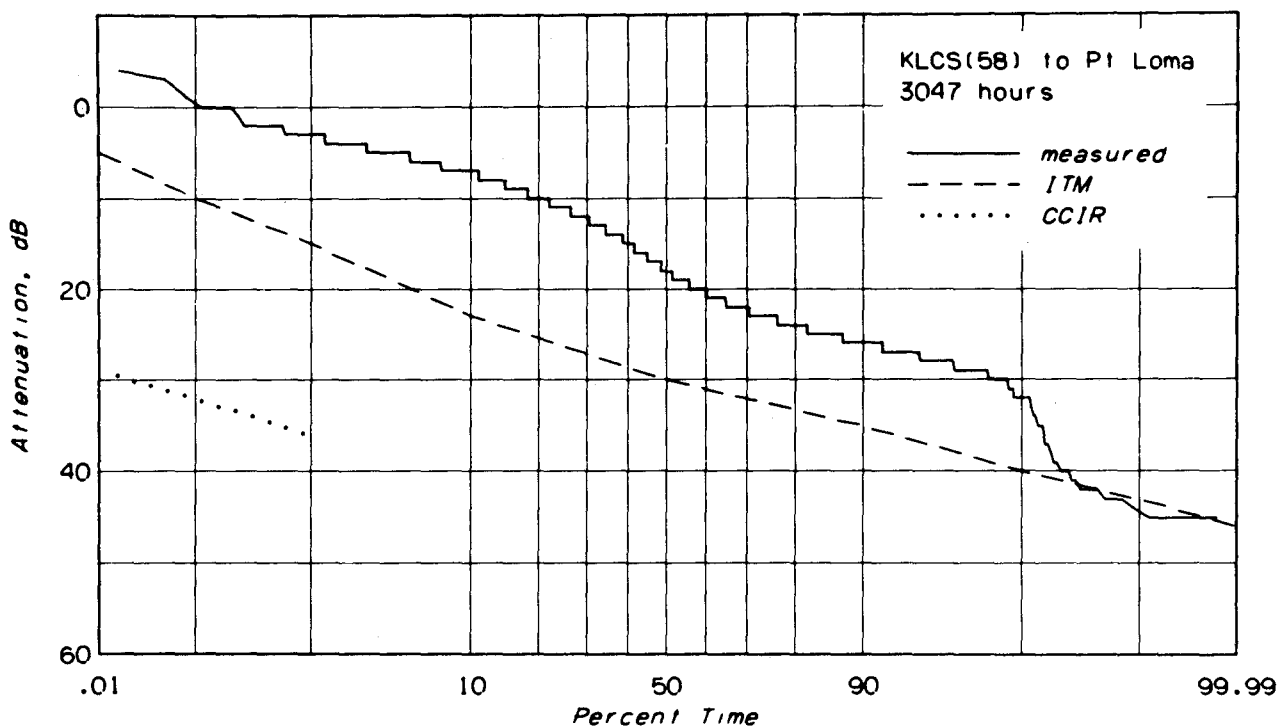on the path from KABC(7) to Point Loma.

Figure 25.   Cumulative distribution of the hourly median data obtained
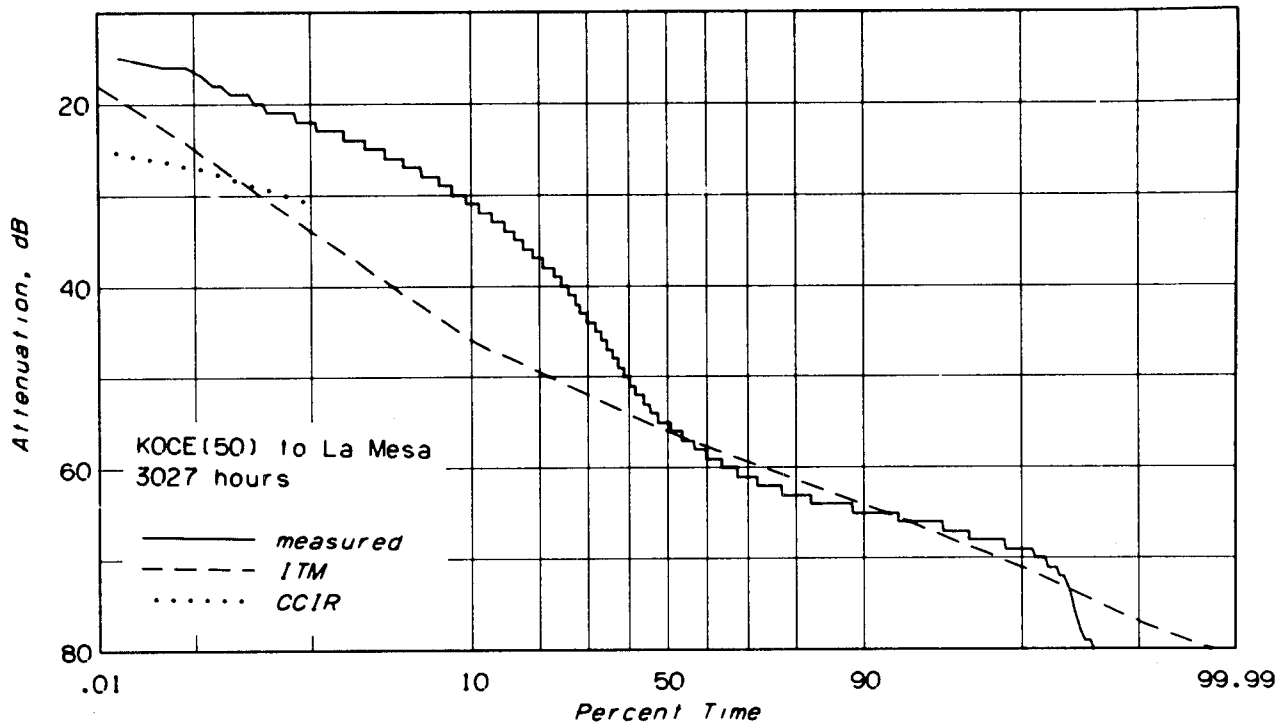on the path from KLCS(58) to Point Loma.

Figure 26. Cumulative distribution of the hourly median data obtained
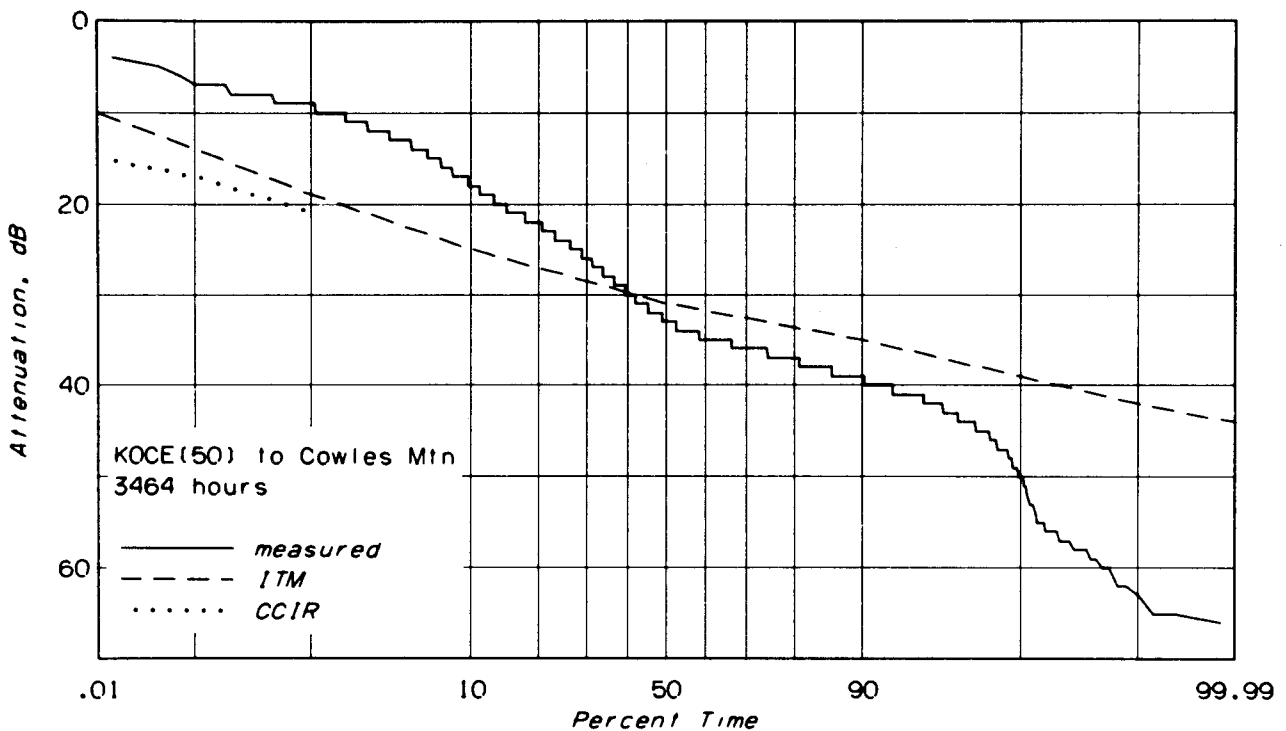on the path from KOCE(50) to La Mesa.

Figure 27. Cumulative distribution of the hourly median data obtained
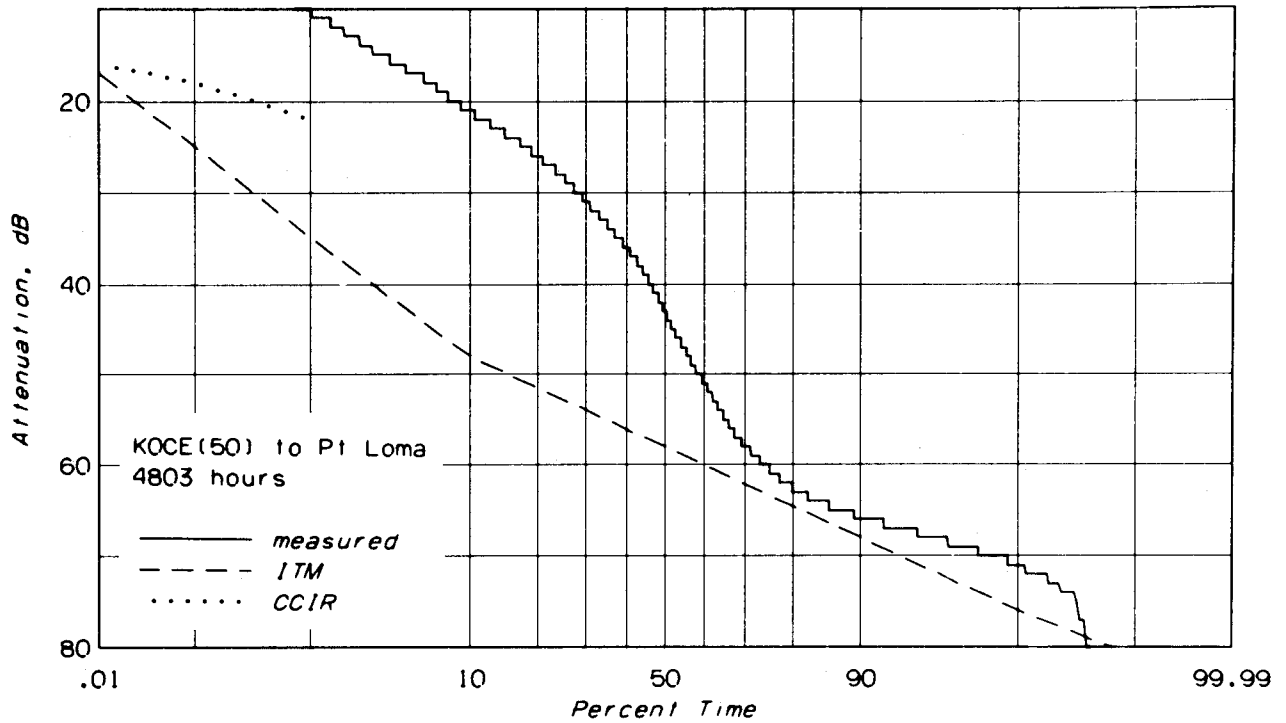on the path from KOCE(50) to Cowles Mountain.

Figure 28. Cumulative distribution of the hourly median data obtained on the path from KOCE(50) to Point Loma.
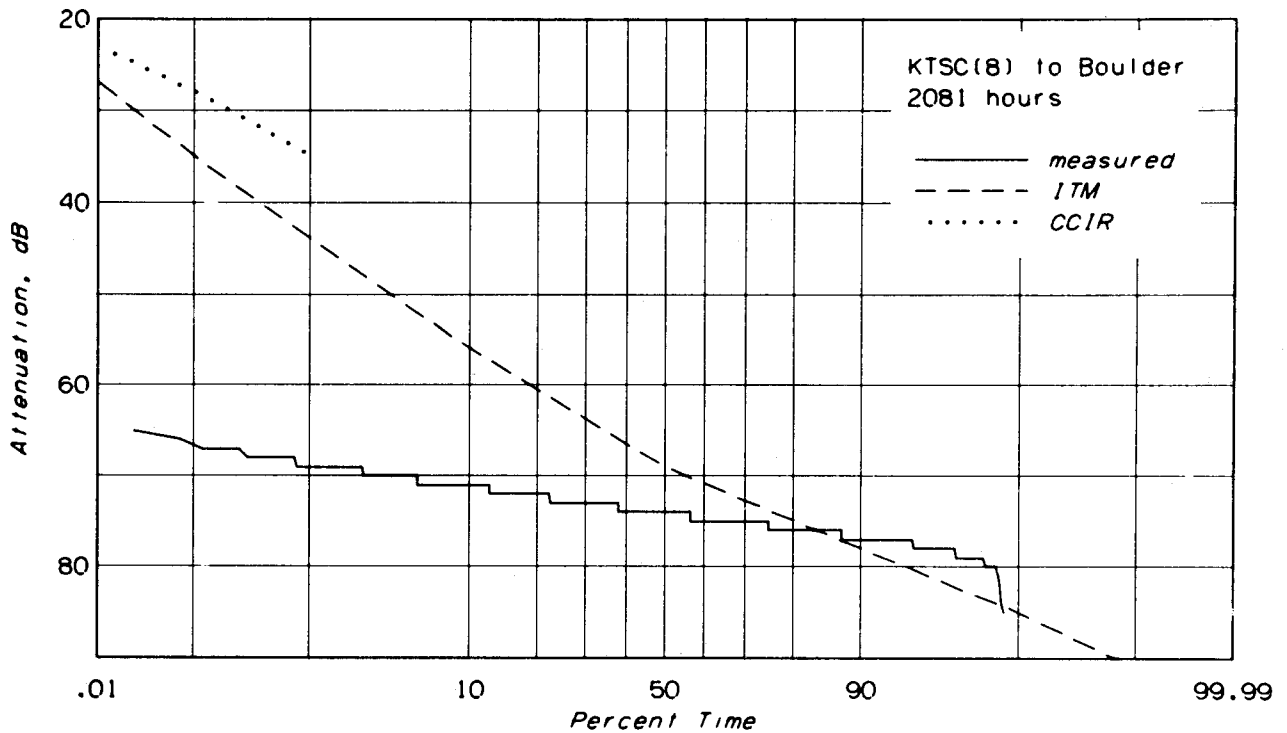

Figure 29. Cumulative distribution of the hourly median data obtained on the path from KTSC(8), Pueblo, to Boulder.

Cumulative distributions corresponding to the eight paths from Mount Wilson are in Figures 18 through 25. It is somewhat surprising that the extrapolated CCIR method seems fairly accurate for the Channel 7 paths but ridiculously low for the five UHF paths. The reason the predicted signal levels are low appears to be the high value used for the terrain irregularity parameter Δh, and clearly, since the direct ray passes well above most of the more rugged parts of the terrain, this irregularity should have little to do with the actual received levels. Indeed, a later version of this method (CCIR, 1982) has almost removed this parameter from consideration.

One expects a path in southern California to be involved in two or more propagation modes because there will be times when a strong super-refractive layer is present and times when it is not; and perhaps there will be times when such a layer lies above the path and times when it lies below. Each propagation mode will have its own statistics and the combination into one cumulative distribution ought to show up as somewhat segmented. Note that atmospheric layers will sometimes give rise to enhanced fields that should displace the small percentiles upward, and that also they may introduce radio holes and suppressed fields and so displace the large percentiles downward.

Mixed mode behavior seems consistent with several of the observed cumulative distributions. For example, the paths from KOCE (in Figures 26, 27, and 28) have distributions with definitely changing slopes. These are paths that we have already indicated were probably particularly sensitive to the presence of layers. The distribution in Figure 23 also seems to involve different modes of propagation. That in Figure 22, however, appears to be a pure straight line. But these two paths are physically almost identical, their only difference being a minor change in frequency. Why their signal-level distribution should be so qualitatively different is a puzzling question. Our own suspicion is that the answer lies merely in the difference between the hours of operation of the two stations.

Variability in the southern California paths can often be very large. The cumulative distributions of hourly medians sometimes have ranges of more than 70 dB. On the other hand, when we look at the eastern Colorado path in Figure 29, we find an extremely flat distribution with an interdecile range of only 6 dB. One probable reason for this is the thin atmosphere in Colorado; but another reason is perhaps that the odd terrain profile in Figure 15 causes the path to behave like a knife-edge path. It is known (see, e.g., Barsis and

Kirby, 1961) that such paths often exhibit a reduced variability. Of course, counterexamples also abound: the KOCE to Cowles Mountain path in Figures 13 and 27 is very clearly a knife-edge path but the observed signal-level distribution is certainly a steep one.

For some of our recently acquired data, the present radio propagation models seem already adequate; for others the differences are large but explainable. Yet others probably require further study. But to us it seems the difficult problem, and the problem needing immediate study, is that of predicting for a given path into which of these simple classifications it will fall--i.e., whether it will fit present models or will "need explanation."

4. ACKNOWLEDGMENTS

5. REFERENCES

Abramowitz, M., and I. A. Stegun (1964), Handbook of Mathematical Functions, N.B.S. Applied Mathematics Series 55 (U.S. Government Printing Office, Washington, D.C. 20402).

Barsis, A. P., and R. S. Kirby (1961), VHF and UHF signal characteristics observed on a long knife-edge diffraction path, J. Research NBS 65D (Radio Prop), pp. 437-448.

CCIR (1978a), Propagation data required for trans-horizon radio-relay systems Doc. XIVth Plenary V, Report No. 238-3.

CCIR (1978b), The evaluation of propagation factors in interference problems at frequencies greater than 0.6 GHz, Doc. XIVth Plenary V, Report No. 569-1.

CCIR (1982), The evaluation of propagation factors in interference problems between stations on the surface of the Earth and frequencies above about 0.5 GHz, Doc. XVth Plenary V, Report No. 569-2.

Dougherty, H. T. (1968), A survey of microwave fading mechanisms, remedies, and applications, ESSA Technical Report ERL 69-WPL4 (NTIS Access. No. COM-71-50288) (see especially p. 42).

Dougherty, H. T., and E. J. Dutton (1981), The role of elevated ducting for radio service and interference fields, NTIA Report 81-69 (NTIS Access. No. PB 81-206138).

Hufford, G. A., A. G. Longley, and W. A. Kissick (1982), A guide to the use of the ITS Irregular Terrain Model in the area prediction mode, NTIA Report 82-100 (NTIS Access. No. PB 82-217977).

Longley, A. G., R. K. Reasoner, and V. L. Fuller (1971), Measured and predicted long-term distributions of tropospheric transmission loss, Office of Telecommunications Report TRER 16 (NTIS Access. No. COM-75-11205).

Longley, A. G., and P. L. Rice (1968), Prediction of tropospheric radio transmission loss over irregular terrain--a computer method 1968, ESSA Tech. Report ERL 79-ITS 67 (NTIS Access. No. AD-676-874).

Misme, P. (1974), Affaiblissement de transmission en propagation guidée par conduit atmosphérique, Annales des télécommunications 29, pp. 105-114.

Norton, K. A., L. E. Vogler, W. V. Mansfield, and P. J. Short (1955), The probability distribution of the amplitude of a constant vector plus a Rayleigh-distributed vector, Proc. IRE 43, pp. 1354-1361.

Rayleigh, Lord (1894), The Theory of Sound, second edition, vol. 1, ch. 2 (republished in 1945 by Dover Publications, New York).

41

Rice, P. L., A. G. Longley, K. A. Norton, and A. P. Barsis (1967), Transmission loss predictions for tropospheric communication circuits, NBS Tech. Note 101, Vols. I and II. (NTIS Access. Nos. AD-687-820 and AD-687-821).

Shkarofsky, I.P., and S. B. Nickerson (1982), Computer modeling of multipath propagation: Review of ray-tracing techniques, Radio Sci. $\underline{17}$, pp. 1133-1158 (see especially p. 1137).

Weibull, W. (1951), A statistical distribution function of wide applicability, J. Appl. Mech. $\underline{18}$, pp. 293-297.

BIBLIOGRAPHIC DATA SHEET

1. PUBLICATION NO. NTIA Report 85-177	2. Gov't Accession No.	3. Recipient's Accession No.

4. TITLE AND SUBTITLE A Study of Interference Fields in a Ducting Environment	5. Publication Date June 1985
	6. Performing Organization Code

7. AUTHOR(S) George A. Hufford and Donald R. Ebaugh, Jr.	9. Project/Task/Work Unit No. 9108102
8. PERFORMING ORGANIZATION NAME AND ADDRESS U.S. Department of Commerce National Telecommunications & Information Admin. Institute for Telecommunication Sciences Boulder, Colorado 80303	10. Contract/Grant No.

11. Sponsoring Organization Name and Address	12. Type of Report and Period Covered
	13.

14. SUPPLEMENTARY NOTES

15. ABSTRACT *(A 200-word or less factual summary of most significant information. If document includes a significant bibliography or literature survey, mention it here.)*

In a cooperative program, the Federal Communications Commission and the Institute for Telecommunication Sciences have begun a study of the interference fields that may arise in a ducting environment. This report gives some preliminary thoughts on how enhanced signal levels might be modeled and describes a measurement program that operated in Southern California. Comparisons are made between some of the first-order statistics of the data and two of the possible models and show that there still remains a large gap between our modeling abilities and reality.

16. Key Words *(Alphabetical order, separated by semicolons)*

Key words: long-term variability; radio ducts; radio propagation; short-term variability; UHF; VHF

17. AVAILABILITY STATEMENT ☒ UNLIMITED. ☐ FOR OFFICIAL DISTRIBUTION.	18. Security Class. *(This report)* Unclassified	20. Number of pages 42
	19. Security Class. *(This page)* Unclassified	21. Price: